Volume n° 2 - from B16 to B33

32nd INTERNATIONAL GEOLOGICAL CONGRESS

THE NEAPOLITAN ACTIVE VOLCANOES (VESUVIO, CAMPI FLEGREI, ISCHIA): SCIENCE AND IMPACT ON HUMAN LIFE

Leader:
G. Orsi

Associate Leaders:
S. de Vita, M.A. Di Vito, R. Isaia

Field Trip Guide Book - B28

Florence - Italy
August 20-28, 2004

Pre-Congress B28

The scientific content of this guide is under the total responsibility of the Authors

Published by:
APAT – Italian Agency for the Environmental Protection and Technical Services - Via Vitaliano Brancati, 48 - 00144 Roma - Italy

Series Editors:
Luca Guerrieri, Irene Rischia and Leonello Serva (APAT, Roma)

English Desk-copy Editors:
Paul Mazza (Università di Firenze), Jessica Ann Thonn (Università di Firenze), Nathalie Marléne Adams (Università di Firenze), Miriam Friedman (Università di Firenze), Kate Eadie (Freelance indipendent professional)

Field Trip Committee:
Leonello Serva (APAT, Roma), Alessandro Michetti (Università dell'Insubria, Como), Giulio Pavia (Università di Torino), Raffaele Pignone (Servizio Geologico Regione Emilia-Romagna, Bologna) and Riccardo Polino (CNR, Torino)

Acknowledgments:
The 32nd IGC Organizing Committee is grateful to Roberto Pompili and Elisa Brustia (APAT, Roma) for their collaboration in editing.

Graphic project:
Full snc - Firenze

Layout and press:
Lito Terrazzi srl - Firenze

Volume n° 2 - from B16 to B33

32nd INTERNATIONAL GEOLOGICAL CONGRESS

THE NEAPOLITAN ACTIVE VOLCANOES (VESUVIO, CAMPI FLEGREI, ISCHIA): SCIENCE AND IMPACT ON HUMAN LIFE

EDITORS:
G. Orsi[1], S. de Vita[1], M.A. Di Vito[1], R. Isaia[1]
AUTHORS:
D. Andronico[5], R. Avino[1], R. Brown[1], S. Caliro[1], G. Chiodini[1], R. Cioni[3], L. Civetta[2], M. D'Antonio[2], F. Dell'Erba[1], P. Fulignati[3], D. Granieri[1], L. Gurioli[3], P. Marianelli[3], R. Santacroce[3], A. Sbrana[3], R. Sulpizio[4]

[1]Osservatorio Vesuviano - INGV - Italy
[2]Università di Napoli - Italy
[3]Università di Pisa - Italy
[4]Università di Bari - Italy
[5]INGV, Catania - Italy

Florence - Italy
August 20-28, 2004

Pre-Congress

B28

Front Cover:
View of the Neapolitan volcanoes from Ischia (P. Fabris - "Campi Phlegraei" of Lord William Hamilton 1776)

Leader: G. Orsi
Associate Leaders: S. de Vita, M.A. Di Vito, R. Isaia

Introduction

A large number of communities as well as megacities have been growing around and even on active volcanoes. Mostly for soil fertility and abundance of volcanic rocks that are good building material, cities on or near volcanoes have grown and continue to grow. If, as is the case of the Neapolitan area, they are in a temperate climate zone, in both commercially advantageous and strategically favourable areas, despite the hazards, humans find good reasons for settlement and development.

The Neapolitan area has been inhabited since Neolithic times (Orsi et al., 2003). The development of an organized society began with the settlement of Greek colonies in the 8th century BC at Ischia and Cuma, in 680 BC on the Megaride islet and called Parthenope, and in 531 BC at Pozzuoli.

Naples is a very suitable site for a field trip devoted to the illustration of the problems of a megacity in an active volcanic area. In fact, together with its surrounding towns, it has been growing between the Campi Flegrei restless caldera and the Somma-Vesuvius, forming a megacity, which we would like to call «Parthenopean Megacity» (Fig. 1).

Figure 1 - Intense urbanization of the Neapolitan area, from satellite imagery.

This megacity, lying on two active volcanic areas and being densely populated, is one of the best examples of high volcanic risk areas in the world.

Regional geologic setting

The Neapolitan area is located within the Campanian Plain, which is bordered by the Southern Apennines (Fig. 2). This mountain chain results from deformation of the African continental margin and is composed of a variety of Mesozoic and Palaeogenic palaeogeographic domains (D'Argenio et al., 1973). The crust is about 25-30 km thick and composed of a pile of tectonic thrusts made up of Triassic to Pliocene sedimentary rocks (Fig. 2) overlying a crystalline-metamorphic basement. From Miocene to Pliocene time, variable compressional tectonic phases have deformed both the sedimentary rocks and their basement terrain. Since Quaternary times, mostly extensional tectonic phases have generated the present setting of the Campanian area.

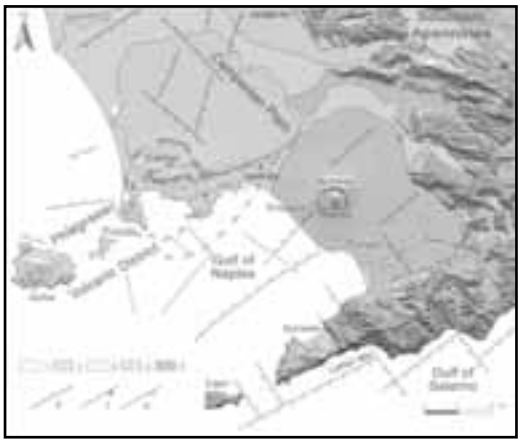

Figure 2 - Geological sketch map of the Neapolitan area. 1) Quaternary and active terrigenous sediments; 2) Somma-Vesuvius volcanics; 3) Phlegraean District volcanics; 4) Pliocene and Miocene terrigenous sediments; 5) Mesozoic carbonate units; 6) faults; 7) overthrusts; 8) caldera margins.

The Campanian Plain, in which lie the active volcanoes, is composed of 2-3,000 m thick sequences of Plio-Quaternary continental, deltaic, and marine sediments, intercalated with volcanic deposits. It is underlain by a graben formed during activation of NW-SE and NE-SW trending normal faults which, at least during Quaternary times (Brancaccio et al., 1991), have downthrown the western Apennines. The regional stress regime, which has determined the formation of the plain, has also favoured generation and rise of the magmas that have fed the recent and active volcanism. Geophysical data and deep wells have shown the presence of volcanic rocks beneath the sediments filling the plain. These rocks have calc-alkaline composition, while those exposed and overlying the sediments are alkaline. The latter belong to the Somma-Vesuvius composite volcano

Volume n° 2 - from B16 to B33

and the Phlegraean Volcanic District, which includes the Campi Flegrei, Ischia and Procida volcanoes. The active volcanoes are Campi Flegrei, Somma-Vesuvius and Ischia; at the island of Procida the last eruption occurred about 18 ka bp.
The Neapolitan area is mostly made up of volcanic rocks and subordinately of shallow-sea, alluvial, coastal and palustrine sediments (Fig. 2). The oldest dated rocks are exposed at Ischia and yield an age of 150 ka. Historical eruptions have occurred at Ischia (from VII century BC to 1302 AD), Campi Flegrei (1538 AD), and Vesuvius (from 79 to 1944 AD).

Somma-Vesuvius. – The Somma-Vesuvius is composed of an older volcano, Mt. Somma, truncated by a summit caldera, and a more recent cone, Vesuvius, within the caldera (Fig. 3).
The growth of the Vesuvius cone took place, although with some minor summit collapses, during periods of persistent low-energy open-conduit activity, the last of which occurred between 1631 and 1944 (Arrighi et al., 2001). The caldera is an elliptical (Fig. 3) complex structure resulting from several collapses, each related to a Plinian eruption (Cioni et al., 1999).

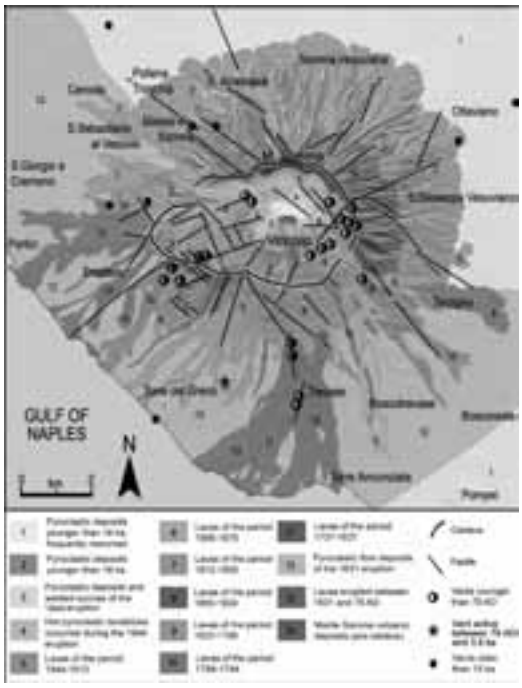

Figure 3 - Somma-Vesuvius geological sketch map (after Orsi et al, 2003. Structural lineaments are after Ventura et al., 1999).

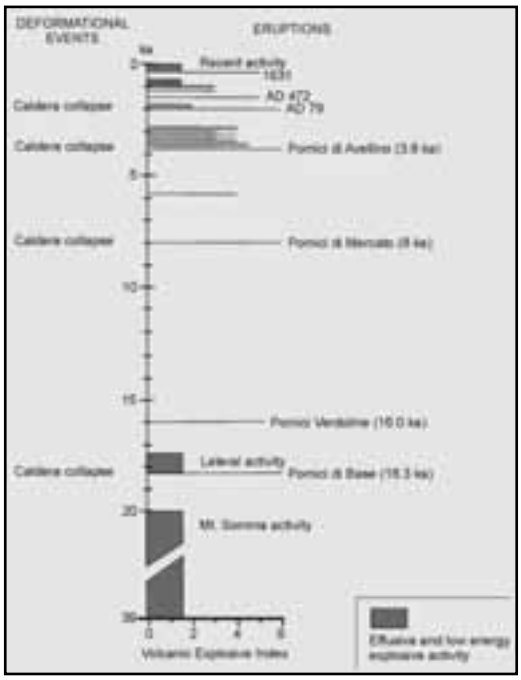

Figure 4 - Chronogram of volcanic and deformational history of Somma-Vesuvius (after Orsi et al., 2003).

The northern portion of the caldera margin is a 300 m high scarp, while the southern portion has been filled by lava flows, which covered the southern slopes of the Mt. Somma as far as the seacoast.
Volcanism in the Somma-Vesuvius area has been active since at least 400 ka bp as testified by volcanic rocks drilled at 1,350 m depth (Brocchini et al., 2001). The Somma volcano formed after the Campanian Ignimbrite eruption of Campi Flegrei (39 ka; De Vivo et al., 2001) (Fig. 4) and its activity was mostly effusive and subordinately explosive, with low energy events (Cioni et al.,1999). The history of the volcano has been characterised either by long quiescence periods, interrupted by Plinian or sub-Plinian eruptions, or by periods of persistent volcanic activity (Fig. 4), with lava effusions and Strombolian to phreato-magmatic eruptions, related to the alternation of closed and open conduit conditions, respectively (Civetta and Santacroce, 1992).
The earliest known Plinian eruption (Pomici di Base; 18.3 ka; Cioni et al., 1999 and references therein) determined the beginning of both the collapse of the Mt. Somma volcano and the formation of the caldera. The Pomici di Base eruption was followed by eruption of lavas that flowed along the eastern slopes

of the volcano, and a quiescent period interrupted 15 ka bp by the sub-Plinian eruption of the Pomici Verdoline (Cioni et al., 2003 and references therein). The subsequent long period of quiescence, during which only two low-energy eruptions took place, lasted until 8 ka bp, when it was broken by the Plinian Mercato eruption (Cioni et al., 1999 and references therein). During the following period of quiescence, interrupted only by two low-energy eruptions, a thick paleosol formed. This paleosol contains many traces of human occupation until the Early Bronze age, and is covered by the deposits of the Plinian Avellino eruption (Cioni et al., 1999 and references therein). This eruption was followed by at least 8 Strombolian to sub-Plinian eruptions, over a relatively short time, and by no less than 7 centuries of quiescence, broken by the Plinian AD 79 eruption (Cioni et al., 1999 and references therein). After this eruption, the volcano generated only two more sub-Plinian events in AD 472 (Rosi and Santacroce, 1983) and 1631 (Rolandi et al., 1993b; Rosi et al., 1993), and low-energy open-conduit activity between the 1st and 3rd, 5th and 8th, 10th and 11th centuries, and 1631 and 1944 (Arrighi et al., 2001). Since the last eruption of 1944, Vesuvius is quiescent, as it has not shown signs of unrest and only moderate seismicity and fumaroles testify its activity.

All Plinian eruptions are characterised by a vent opening, a sustained column and pyroclastic flow and/or surge phases, and are accompanied by volcano-tectonic collapses. Sustained columns, which reach maximum heights of about 30 km, generate widespread fallout deposits (1.5-4.4 km^3, DRE) (Fig. 5).

Pyroclastic currents (0.25 and 1 km^3, DRE) are distributed along the volcano slopes and within the surrounding plains, reaching maximum distances of over 20 km from the vent. In proximal areas, thick breccia deposits are related to caldera collapse. The quiescence periods preceeding the Plinian eruptions last from several centuries to millennia (Fig. 4)

Among the sub-Plinian eruptions of Vesuvius, only the AD 472 and the 1631 events are studied in detail (Rosi and Santacroce, 1983; Rolandi et al., 1993; Rosi et al., 1993). They are characterised by the alternation of sustained columns and pyroclastic flow and/or surge generation. Sustained columns are less than 20 km high and pyroclastic currents travel distances not in excess of 10 km.

Fallout deposits of both Plinian and sub-Plinian eruptions are dispersed to the east of the volcano

Vesuvius is located at the intersection of NW-SE and NE-SW oriented fault systems. The results of seismic investigations, constrained by one deep drilling (Zollo et al., 2002) show that the shallow structure of Vesuvius comprises 1.5-2 km of interbedded lavas and volcaniclastic, marine, and fluvial sedimentary rocks of Pleistocene age. A high velocity body, likely to be a sub-volcanic structure, is under the summit caldera. The top of the Mesozoic limestone basement is at 2.5-3 km of depth. The occurrence of a high-P wave velocity zone beneath the volcano, which extends from about 0.5 to 2-3 km of depth, as well as of local volcano-tectonic seismicity shallower than 6-7 km of depth (Bianco et al., 1998), indicate that it is extremely unlikely that shallow magmatic reservoirs of significant size (>1 km in diameter) occur in the 0-7 km range of depth. Furthermore, the results of a seismic tomography study (Auger et al., 2001) identify a horizontal low-velocity layer with its flat top at about 8 km beneath the volcano. This is interpreted as the top of the present magma

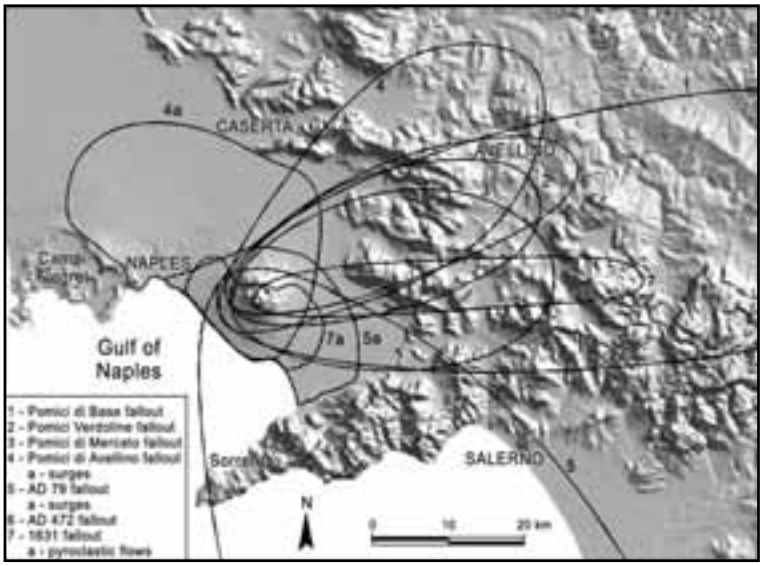

Figure 5 - Distribution of Plinian and sub-Plinian deposits of Somma-Vesuvius eruptions.

reservoir. This depth coincides with the upper portion of a zone of clinopyroxene crystallization, indicated by fluid inclusion data (Belkin et al., 1985; Marianelli et al., 1995; 1999). The Moho discontinuity in the Vesuvius area is at a depth of 29-30 km (Gasparini et al., 2001).

In its history Somma-Vesuvius has erupted about 50 km^3 of magma of varying composition. According to the different degrees of silica under-saturation of the erupted magmas, it is possible to distinguish three periods of activity (Santacroce, 1983). The oldest, from ca. 39 to 11.5 ka bp, is characterised by emission of slightly under-saturated lavas, of variable composition from K-basalt to K-trachyte. The second period, from 8 ka bp to AD 79, is characterised by the emission of products varying in composition from tephrite to phonolite. The products of the last period, from AD 79 to AD 1944, range from leucititic tephrite to leucititic phonolite.

All these products show a range of Sr-Nd-Pb isotopic compositions (D'Antonio et al., 2004 and references therein): $^{87}Sr/^{86}Sr$ ratio ranges between 0.7066 and 0.7080; $^{143}Nd/^{144}Nd$ ratio ranges from 0.5126 to .5124; Pb isotope ratio show smaller ranges (e.g. of values for $\delta^{18}O$ (7.3-11.4‰) is reported (Ayuso et al., 1998 and references therein), whereas $^3He/^4He$ ratios are clustered around 2.4 R/R_a (Graham et al., 1993). Sr and Nd isotopes of the Plinian and Strombolian products show a variation through time, with increasing or decreasing $^{87}Sr/^{86}Sr$ ratio (and the

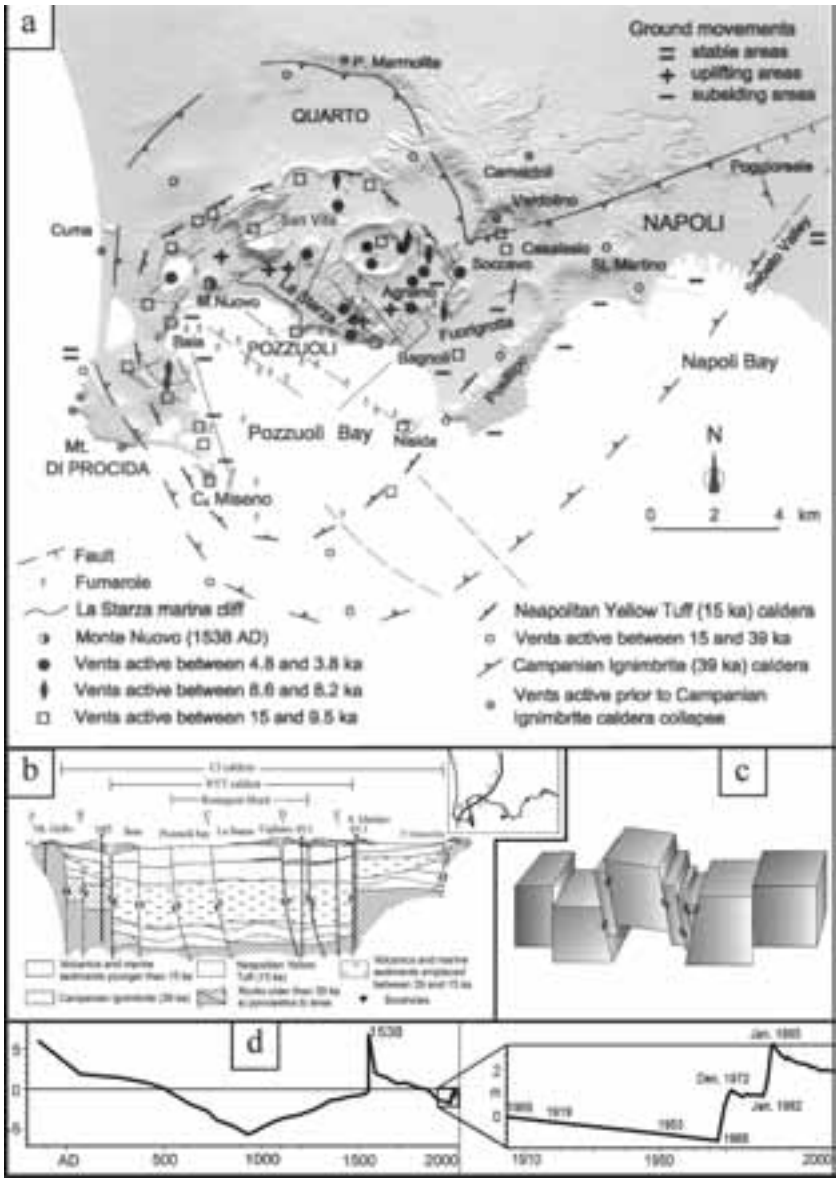

Figure 6 - a) Structural map of the Campi Flegrei caldera; b) SW-NE cross section (location is shown in the insert); c) simple-shearing block resurgence model for the caldera complex; d) vertical ground movements at Serapis Roman market in Pozzuoli.

Figure 7 - Chronogram of volcanic and deformational history of the Campi Flegrei caldera (after Orsi et al., 2003).

opposite for Nd isotopes) from the first to the last erupted magma. Strong isotopic disequilibria occur among minerals and between minerals and glass. The Sr- and Nd-isotopes have been used to investigate the processes in the magma reservoirs. The isotope and geochemical data for Plinian eruption products evidence that the magma chamber(s) feeding Plinian eruptions (3-5 km depth; Barberi et al., 1981) are refilled by isotopically distinct, mafic, high-T (>1150 °C) magma batches rising from depths of 10-20 km (Cioni et al., 1999 and references therein), where mantle-derived magmas stagnate, differentiate and probably are contaminated by continental crust.

The deep magma batches, through crystallization and mixing with the shallow portions of the feeding systems, generate isotopically and geochemically layered reservoirs. On the contrary, during open conduit conditions the deep, volatile-rich magma batches rise to less than 2 km of depth and mix with the crystal-rich, volatile-poor resident magma, triggering eruptions (Marianelli et al., 1999 and references therein).

<u>*Campi Flegrei caldera*</u> - The Campi Flegrei caldera, the main feature of the Phlegraean Volcanic District, includes a continental and a submerged part. It is a resurgent nested structure (Fig. 6) formed during two major caldera collapses related to the eruptions of the Campanian Ignimbrite (39 ka; Fedele et al., 2003 and references therein) and the Neapolitan Yellow Tuff (15 ka; Deino et al., 2004 and references therein), respectively (Orsi et al., 1996).
The geometry and dynamics of both large calderas, as well as of smaller volcano-tectonic collapses, were deeply influenced by both local and regional stress regimes. Each large collapse affected the structural conditions of the system, and constrained the foci of later volcanism. The age of the beginning of volcanism in the area is not known. The oldest dated volcanic unit yielded an age of 60 ka (Pappalardo et al., 1999) and is related to a volcanism extending beyond the caldera (Fig. 6a)

The Campanian Ignimbrite eruption and caldera collapse was the earliest event to profoundly influence the present geological setting of the area. The Neapolitan Yellow Tuff eruption and caldera collapse was the last dramatic event in the history of the caldera.
After the Neapolitan Yellow Tuff eruption, both volcanism and deformation have been very intense within the caldera (Fig. 6, 7) (Orsi et al., 1999a and references therein). There have been about 70 eruptions, grouped in three epochs of activity (15.0-9.5, 8.6-8.2 and 4.8-3.8 ka), during which eruptions have followed one another at mean time intervals of a few tens of years. The last event was in 1538, after about 3.0 ka of quiescence (Fig. 7), and formed the Mt. Nuovo cone (Di Vito et al., 1987). 64 of these eruptions were phreatomagmatic to magmatic explosive events. Contemporaneous magmatic and phreatomagmatic fragmentation dynamics has been widely recognised and has been demonstrated for the Agnano-Monte Spina eruption (Dellino et al., 2004a and references therein). Only the Pomici Principali (10.3 ka; Di Vito et al., 1999 and references therein) and the Agnano-Monte Spina, occurred during the I and III epochs of activity respectively were of high-magnitude, Plinian eruptions. On the basis of the extent of the area covered by the deposits, considered as indicative of the magnitude, the other explosive events have been subdivided by Orsi et al. (2004) in low- and medium-magnitude eruptions. Fallout deposits of the I epoch covered the north-eastern sector of the caldera and the Camaldoli hill, 15 km from the caldera centre (Fig. 8a). Only beds of the Pomici Principali Tephra are 20 cm thick along the western

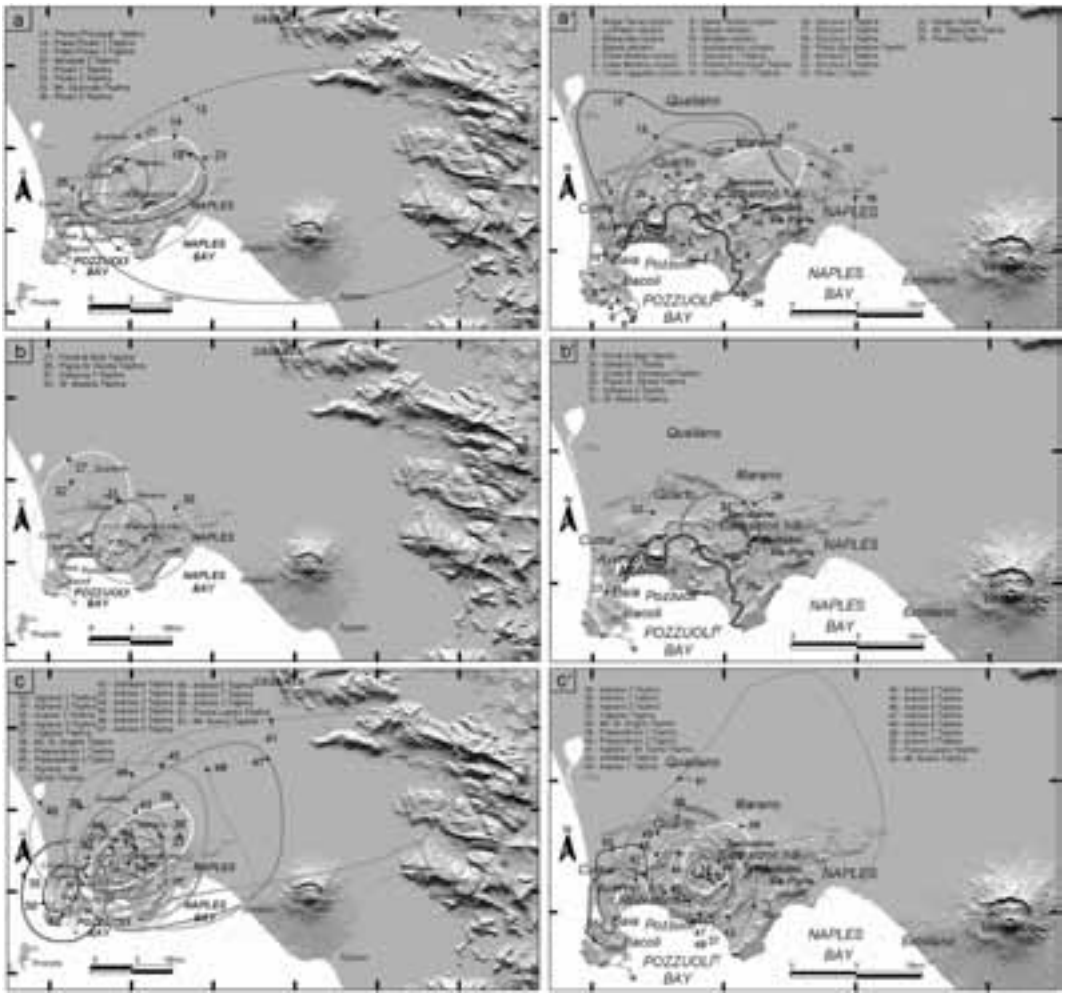

Figure 8 - Distribution of the pyroclastic deposits of the past 15 ka at the Campi Flegrei caldera. a, b and c: 10-cm isopachs of fallout deposits of the I, II and III epoch, respectively; a', b' and c': areal distribution of pyroclastic-current deposits of the I, II and III epoch, respectively.

margin of the Apennines, at about 50 km from the vent. Pyroclastic currents travelled within the caldera floor and reached the Campanian plain. The eruptions of the II epoch were all low-magnitude events. Fallout deposits covered only the caldera and its immediate surroundings, while most of the pyroclastic currents deposited their load within the caldera lowland (Fig. 8b). The fallout deposits of the III epoch and of the Mt. Nuovo eruption covered the caldera floor and its surroundings (Fig. 8c). Only beds of the Agnano-Monte Spina Tephra covered a large area up to the Apennines. Pyroclastic currents travelled across the caldera floor and subordinately over the northern slopes of the Camaldoli hill (de Vita et al., 1999).

The caldera has been affected by structural resurgence through a simple-shearing mechanism (Orsi et al., 1991) that broke its floor in blocks and caused a maximum net uplift of about 90 m at the La Starza marine terrace (Fig. 6) (Orsi et al., 1996). The distribution of the vents active through time (Fig. 6a) is a good tracer of the structural conditions of the caldera. In fact during both the I and II epochs vents were mostly located along the marginal faults of the Neapolitan Yellow Tuff caldera. Whereas the vents of the III epoch were along the normal faults intersecting the north-eastern portion of the Neapolitan Yellow Tuff caldera floor, in response to the simple-shearing mechanism, established not later than 5 ka bp (Orsi

et al., 1999a).

This mechanism generated a compressive stress regime within the south-western portion of the caldera floor, the Pozzuoli bay, and a tensile stress regime within the north-eastern portion, the area between the Agnano and San Vito plains (Fig. 6). Only Averno 1 and 2, and Mt. Nuovo eruptions occurred in the sector where the two fault systems delimiting the resurgent block north-westward, intersect.

During the past 2.0 ka, the floor of the caldera has been affected by ground movement, documented at the Serapis Roman market in Pozzuoli (Fig. 6d). Since late 1960s, unrest episodes have been documented by the monitoring system in 1969-72, 1982-84, 1989, 1994 and 2000, and have generated uplifts of 170, 180, 7, 1 and 4 cm, respectively. Geometry of these short-term deformation events are very similar to that of the long-term deformation. This element, together with the earthquake focal mechanisms, suggest that also the unrest episodes occur through a simple-shearing mechanism. Therefore they are likely to be transient events during the long-term deformation and reflect the stress regime within the caldera, which has not changed at least over the past 5 ka (Orsi et al., 1999a).

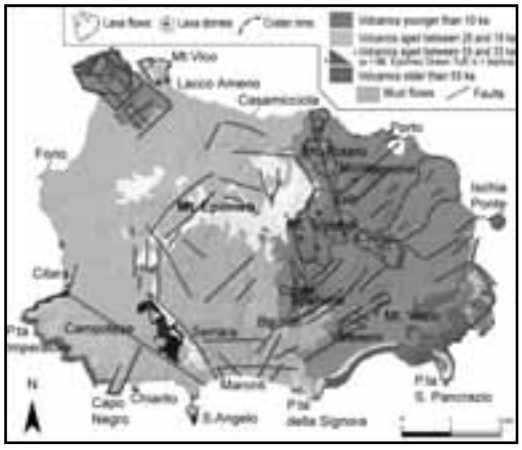

Figure 9 - Geological sketch map of Ischia (after Orsi et al., 2003).

The magmas erupted at Campi Flegrei range in composition from trachybasalt to phono-trachyte, with a predominance of trachyte (D'Antonio et al., 1999 and Pappalardo et al., 1999, and references therein). The less differentiated magmas (trachybasalt and latite) erupted between 10 and 8 ka along NE-SW regional tectonic structures (Orsi et al., 1996).

Seismic data show that beneath the Campi Flegrei caldera, the top of the Mesozoic limestone basement occurs at about 4 km depth (Zollo et al., 2003), above which no evidence of magma reservoirs of significant size has been found. Melt inclusion data indicate zones of clinopyroxene and olivine crystallization between 10 and 20 km depth, suggesting the presence of deep magma reservoirs (Cecchetti et al., 2001), at the same depth of those estimated for Vesuvius. The depth of the Moho below the Phlegraean Volcanic District is of about 25 km (Ferrucci et al., 1989).

The Campi Flegrei rocks exhibit a wide range of $^{87}Sr/^{86}Sr$ (0.7068-07086), but limited ranges of $^{143}Nd/^{144}Nd$ (0.51240-0.51266) and Pb-isotope ratios (e.g. $^{206}Pb/^{204}Pb$: 18.85-19.25; Pappalardo et al., 2002a, b and references therein). Wide ranges of $\delta^{18}O$ (Turi and Taylor, 1976) and $\delta^{11}B$ (Tonarini et al., 2004) have also been measured.

Variations of Sr, Nd and Pb isotope ratios of magmas erupted since 60 ka illustrate the history of the Campi Flegrei magmatic system. $^{87}Sr/^{86}Sr$ increases from 60 to 44 ka, is constant from 44 to 17 ka, increases again at 15 ka, prior to the Neapolitan Yellow Tuff eruption, and then exhibits a wide range, between 0.7073 (value characteristic of Campanian Ignimbrite) and 0.7086. The increase of $^{87}Sr/^{86}Sr$ is associated with a decrease in the Nd isotope ratio. According to the isotopes-time correlation, Pappalardo et al. (2002b) have identified four groups of magmas: 1) trachytic magmas erupted before Campanian Ignimbrite ($^{87}Sr/^{86}Sr$ ca. 07068); 2) Campanian Ignimbrite trachytic magmas ($^{87}Sr/^{86}Sr$ ca. 0.7073); 3) Neapolitan Yellow Tuff latitic to trachytic magmas ($^{87}Sr/^{86}Sr$ ca. 0.70755); 4) shoshonitic magmas erupted for the first time at ca. 10 ka ($^{87}Sr/^{86}Sr$ ca. 0.708) along portions of regional faults. The shoshonitic magmas contain xenoliths and xenocrysts of probable crustal origin, enriched in radiogenic Sr ($^{87}Sr/^{86}Sr$ up to 0.711; Pappalardo et al., 2002b). Mixing/mingling among the four components can explain all the isotopic variations of the post-Neapolitan Yellow Tuff products.

The structure of the magmatic system is, therefore, characterised by a deep reservoir extending between 20 and 10 km depth, where mantle derived magma stagnate and eventually are contaminated by continental crust (Pappalardo et al., 2002b). From the deep reservoir, magmas rise to shallow depth, where they either form large chambers, or reach the surface through regional faults along which they mix with residual melts.

Volume n° 2 - from B16 to B33

Ischia - The island of Ischia, the emerged top of a large volcanic complex rising more than 1,500 m above sea floor, is an active volcanic field that covers an area of about 46 km^2 and is dominated by Mt. Epomeo (787 m a.s.l.). Ischia is composed of volcanic rocks, landslide deposits, and subordinate terrigenous sediments (Fig. 9). The volcanic rocks range in composition from trachybasalt to phonolite; the most abundant are trachyte and alkali-trachyte. Volcanism began more than 150 ka bp (Vezzoli, 1988) and continued until the last eruption of 1302 AD (Fig. 10).

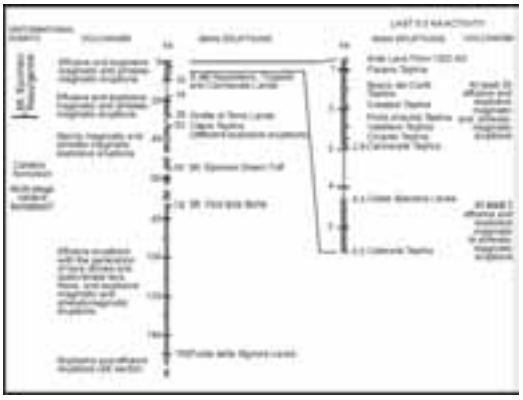

Figure 10 - Chronogram of volcanic and deformational history of Ischia.

The oldest rocks are exposed in the south-eastern part of the island and belong to a partially exposed volcanic complex. The products of the volcanism between 150 and 74 ka bp, are small trachytic and phonolitic domes at the periphery of the island. A poorly defined period of pyroclastic activity followed, predating the large Mt. Epomeo Green Tuff caldera-forming eruption (55 ka). Lacking a detailed stratigraphic and compositional study on the volcanics aged between 74 and 55 ka, volcanism in the past 55 ka has been tentatively subdivided into three periods of activity (Civetta et al., 1991).

The Mt. Epomeo Green Tuff consists mostly of trachytic ignimbrites that partially filled a depression invaded by the sea in what is now the central part of the island. The caldera collapse was followed by the Mt. Epomeo block resurgence, which occurred through a simple-shearing mechanism (Fig. 6c) and determined a net uplift of about 900 m (Orsi et al., 1991). Volcanism continued with a series of hydromagmatic and magmatic explosive eruptions of trachytic magmas up to 33 ka. Most of the vents were located along the present south-western and north-western periphery of the island.

After a 5 ka long period of quiescence, volcanism resumed at about 28 ka with the eruption of trachybasaltic magma along the south-eastern coast, and then continued sporadically until 18 ka. Hydromagmatic and magmatic explosive eruptions along the southern coast mostly erupted alkali-trachytic magmas, while effusive eruptions formed trachytic lava flows.

The most recent period of activity began at about 10 ka. Volcanism has been mainly concentrated in the past 2.9 ka, with almost all the vents in the eastern part of the island (Sansivero, 1999). Only a few were outside this area, along regional faults. They generated a lava field, in the north-western corner of the island, and a pyroclastic sequence in the south-western part. At least 35 effusive and explosive eruptions took place. Effusive eruptions emplaced lava domes and high-aspect ratio lava flows. Explosive eruptions, both magmatic and phreatomagmatic, generated tuff cones, tuff rings and variably dispersed pyroclastic-fall and -flow deposits. Emplacement of landslide and mudflow deposits prior and after these eruptions testifies ground deformation, and are likely to be related to resurgence.

Geological and petrological data, as well as the results of modelling of magnetic data (Orsi et al., 1999b), suggest that the magmatic system of Ischia is presently composed of a deep and poorly-evolved magma reservoir, interconnected with shallower, smaller and more-evolved magma batches, which have fed the recent activity.

The magmas erupted at Ischia have a wide range of isotopic values: $^{87}Sr/^{86}Sr$ ratio varies between 0.7058 and 07073, while $^{143}Nd/^{144}Nd$ ratio varies between 0.51246 and 0.51261 (Civetta et al. 1991b); $^{206}Pb/^{204}Pb$ ratio varies between 18.88 and 19.05 (Arienzo et al., 2004); δO^{18} varies between 6.14 and 6.99. The Sr isotopic ratios are generally less radiogenic than those of Vesuvius and Campi Flegrei, while the Nd, Pb and B isotopic ratios are similar. Geochemical and isotopical variations through time (Civetta et al., 1991) have evidenced that the magmatic system between 55 and 33 ka acted as a closed system. Before the 28-18 ka period of activity, it was refilled by a deeper less-evolved magma, which progressively mixed with the more-evolved resident magma. The last period of activity was preceded by arrival of new magma. Complex mingling/mixing processes operated till the last eruption, as testified by isotopic and mineralogical disequilibria.

Origin of the Campanian magmas - In agreement with geophysical and geological data on the geodynamics of the Tyrrhenian Sea and the structural setting of Neapolitan volcanoes, the isotopic data (Sr, Nd, Pb, B) (Tonarini et al., 2004; Arienzo et al., 2004; Civetta et al., 2004) suggests the involvement of three components in the genesis and evolution of the feeding magmas: 1) the T-MORB asthenospheric mantle, mostly represented by Tyrrhenian seafloor basalts and, in part, by Procida K-basalts; 2) fluids derived from sediments of the Ionian NW-dipping subduction zone, which progressively modify the mantle wedge in relation to Ischia-Procida and Vesuvius-Campi Flegrei; 3) fluids deriving from the continental crust which contaminate the mantle derived magmas. This last process is operative mostly on the post-39 ka Vesuvius and Campi Flegrei magmas, at a depth between 10 and 20 km, where mineralogical and geophysical data indicate the occurrence of discrete magma reservoirs. From these depths, batches of isotopically distinct magmas rise to shallow reservoirs, where they mix with the resident magma, differentiate and, in cases, can trigger an eruption.

Field itinerary

DAY 1

Stop 1:

The 1944 eruption of Vesuvius and the present Crater

Significance. - The 1944 last eruption of Vesuvius. Evolution of the crater after the 1906 eruption. Physical and socio-economical features.

The 1944 eruption. - The 1944 eruption is the last eruption of the Vesuvius. Since then, the volcano has been quiescent, only fumaroles and moderate seismicity testify its activity. The 1944 eruption closed a cycle of persistent activity, begun in 1914 and characterised by mainly effusive central eruptions. 50-100 millions of m^3 of lavas and pyroclasts had almost completely filled the 1906 eruption crater (720 m wide and 600 m deep).

Imbò (1949) reported a detailed description of the eruption, which is here summarised.

On March 13, the spatter cone, emerging from the crater, began to collapse and seismicity increased. A new cone formed between March 13 and 16 and collapsed on March 17.

Figure 11 - Distribution of the 1944 Vesuvius eruption deposits.

The eruption begun on the afternoon of March 18th with Strombolian activity. A lava flow overflowed out of the northern portion of the crater rim at 4.30 pm, and reached the Valle dell'Inferno at 10.30 pm (Fig. 11).

Other lavas overflowed the southern portion of the rim, almost simultaneously, and the western portion at 11.00 pm, reaching the Fosso della Vetrana at 11.00 am of March 19. From the afternoon of March 20 and for the following night, new lava flows overflowed the northern portion of the crater rim. On March 21st, the southern lava flow stopped at about 300 m a.s.l., while the northern flow reached the towns of S. Sebastiano and Massa di Somma between 1.00 and 2.00 am. The 10,000 inhabitants were evacuated and transferred to Portici. Around 5.00 pm a new phase of the eruption which generated 8 spectacular lava fountains, began and lasted till 00.48 pm of the next day. The last fountain, lasted about 5 hours, reached a height of about 1,000 m. Scoriae and ash fallout beds were laid down southeast of the volcano, between the towns of Angri and Pagani. A large amount of incandescent scoriae, due to the ground movement related to intense seismic tremor, generated hot avalanches which reached the foot of the cone.

At 00.48 pm of March 22nd there was a transition from the lava fountain phase to a buoyant column phase (Fig. 12). The convective portion of this column, 5-6 km high, was dispersed towards south-east. Partial collapses generated pyroclastic currents which moved along the slopes of the cone. This eruption phase, during which the crater enlarged progressively, was characterised by intense seismic tremor. On March

Figure 12 - Buoyant column phase of the 1944 Vesuvius eruption.

Figure 13 - Partial column collapse with generation of pyroclastic currents during the 1944 Vesuvius eruption.

23 a new and last phase began. It was dominated by phreatomagmatic explosions with energy decreasing through time. Also seismicity changed from tremor to discrete shocks. The ash-rich columns were directed towards the south-south-west, and small pyroclastic currents flowed on the slopes of the cone (Fig. 13). The eruption ended on March 29.

The 1944 products range in composition from phonolitic tephrite to tephrite. The lower portion of the pyroclastic sequence includes both brownish vesicular and dark dense lapilli juvenile clasts. The two types of clasts, petrographically and chemically similar, differ for vesicularity, matrix colour (yellowish to brownish) and crystallinity. The upper portion of the sequence includes only denser juvenile clasts, rich in clinopyroxene.
Phenocrysts content increases and vesicularity decreases up-section. Clinopyroxene is ubiquitous phenocryst phase and occurs in two varieties, a colourless diopside and a greenish salite. Leucite, plagioclase, biotite and olivine occur as phenocrysts and in glassy groundmass during the whole sequence, in varying proportions. Leucite at the base and clinopyroxene and olivine upward occur as loose megacrysts during the whole sequence.
K-phonotephritic magma was emitted during the effusive phase and the first lava fountain, whereas strongly porphyritic K-tephritic magma was extruded during the most intense fountain. Melt inclusions compositions (major and volatile elements) highlight that the erupted magmas underwent differentiation at different pressures. The K-tephritic volatile-rich magma (up to 3wt.% H_2O, 3.000 ppm CO_2 and 0.55wt. % Cl) evolved to a K-phonotephritic melt through crystallization of diopside and forsteritic olivine at total fluid pressure >300 MPa. This magma fed a very shallow reservoir. The low pressure differentiation of the volatile-poor K-phonotephritic magmas (H_2O less than 1wt.%) involved mixing, open-system degassing, and crystallization of leucite, salite, and plagioclase. The eruption was triggered by intrusion of a volatile-rich magma rising from a depth of 11-22 km into the shallow magma chamber. The lava effusion phase of the eruption partially empted the shallow reservoir, the top of which is within the caldera edifice. The newly arrived magma mixed with that resident in the shallow reservoir and forced the transition to the lava fountain phase.
The pyroclastic deposits contain lithics of skarn and other thermo-metamorphic rocks, grouped in four main lithotypes: metasomatised cumulites, Ca-skarn, Mg-skarn and cornubianites. These rocks, which could result from an interaction between magma and magma chamber sedimentary wall-rocks (limestones, dolomites, marls and siltites), are particular in this 1944 eruption. Their occurrence suggests that the magma chamber was a high aspect ratio structure, reaching the sedimentary basement of the volcano around 3-4 km of depth. The presence of periclase in the Mg-Skarn could suggest hypo-abyssal conditions with maximum pressures of 1,000 bars.
The most relevant effects of the eruption were: twenty-six people dead in the area affected by lapilli and ash fallout, due to a collapse of the roots; two villages partially destroyed by lava flows; three years of missed crops in the downwind area.

<u>The crater</u> - A complete sequence of the 1914-1944 deposits of the last cycle of activity at Vesuvius is exposed along the north-eastern portion of the crater

Figure 14 - View of the north-eastern portion of the Vesuvius crater.

slope (Fig. 14). The sequence is dominated by lavas, the most significant was extruded on 1929, with minor spatter and scoriae beds. It is horizontal, fills the 1906 eruption crater and unconformably covers the sequence of rocks exposed in the 1906 crater. Both sequences are topped by the deposits of the 1944 eruption in parallel unconformity.

A grey massive lava, the basal unit of the 1944 eruption sequence (Fig. 15), is a continuous layer grading into a densely-welded crudely-stratified spatter succession emplaced during the lava fountaining phase. The largest part of this succession was emplaced during the VIII fountain (7.30 am -00.48 pm, March 22), when concomitance of rapid spatter accumulation and strong seismic tremor, caused hot avalanches. The spatter succession is covered in parallel unconformity by another succession of black and grey scoriaceous lapilli and bomb deposits with interlayered coarse ash

Figure 15 - The 1944 Vesuvius eruption deposits along the northern crater wall.

beds. Variation in deposit characteristics is related to the change in fragmentation dynamics at 00.48 pm, with the formation of a buoyant ashy column.
The upper part of the 1944 sequence is composed of intercalated reddish and violaceous lapilli and bomb deposits, and coarse ash beds, and is topped by grey ash deposits rich in lithic fragments, mainly composed of fresh and hornfelsed lavas. It was deposited during the phreatomagmatic final phase of the eruption.
The Vesuvius fumaroles. - Fumarole activity is widespread in the Vesuvius crater area. Fumaroles of the crater rim and of the inner crater slopes

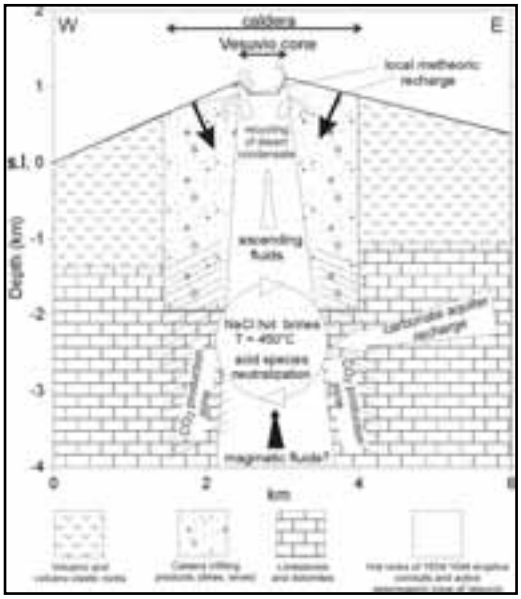

Figure 16 - Geochemical model of the Vesuvius hydrothermal system.

discharge fluids rich in atmospheric gases with outlet temperatures ranging from 60 to 75°C. The fumarolic fluids of the crater bottom (vents FC1, FC2, and FC5) have, instead, typical hydrothermal compositions, with H_2O as a major constituent, followed by CO_2, H_2, H_2S, N_2, CH_4, and CO in order of decreasing concentrations, and undetectable SO_2, HCl, and HF. These fumaroles, whose outlet temperatures have been close to the local water boiling point since 1988, are fed by a hydrothermal system located underneath the crater.
Fumarolic water is either meteoric water enriched in ^{18}O through water-rock oxygen isotope exchange in the hydrothermal environment or a mixture of

Volume n° 2 - from B16 to B33

meteoric and arc-type magmatic water, as indicated by the $\delta^{18}O_{H2O}$ values, suitably corrected for oxygen isotope exchange between H_2O and CO_2, and the δD_{H2O} values. It is equally possible that both water-rock oxygen isotope exchange and addition of magmatic water take place in the hydrothermal system of Vesuvius crater.

Fumarolic CO_2 has a double origin: part of The CO_2 is of deep provenance (magmatic), and part is from metamorphic reactions involving marine carbonates (although addition of a small fraction of magmatic CO_2 cannot be ruled out), as suggested by both the $\delta^{13}C_{CO2}$ values and gas equilibria. The decarbonation reactions result from a local thermal anomaly in the thick carbonate sequence, at >2.5 km underneath the volcano (Chiodini et. al., 2001) (Fig. 16).

Seen the large availability of salts in deep volcanic hydrothermal environments, mainly due to absorption of acid, magmatic gases in deeply circulating ground-

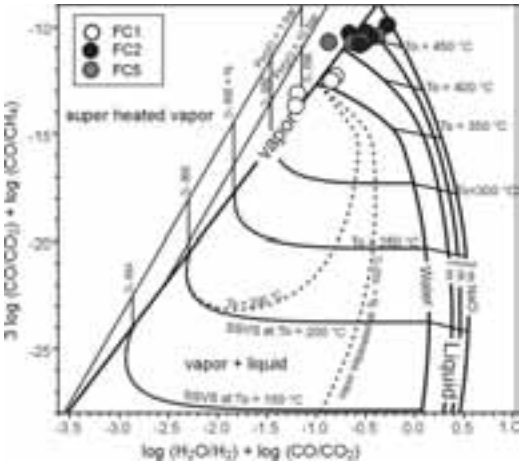

Figure. 17 - Gas equilibria within the H_2O-H_2-CO_2-CO-CH_4 gas system (after Chiodini and Marini, 1998).

waters and the subsequent neutralization of these acidic aqueous solutions through water-rock interaction, it seems likely that NaCl liquids of unknown (probably high) salt content rather than pure water, circulate in the Vesuvius hydrothermal system.

Accepting this hypothesis, gas equilibria was investigated taking into account the solubility of relevant gas constituents in NaCl aqueous solutions of specified concentrations. It turns out that C-H-O gas species equilibrate, probably in a saturated vapour phase, at very high temperatures: 360 to 370°C for vent FC1 and 430 to 445°C for vents FC2 and FC5. The minimum salinity of the liquid phase coexisting with

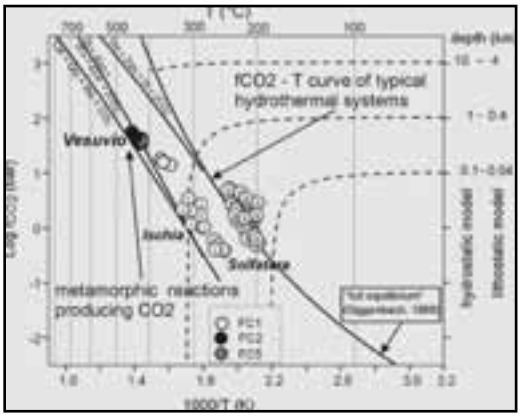

Figure 18 - Carbon dioxide fugacities versus 1000/T (K) diagram. The points of Vesuvius are representative of a very high temperature hydrothermal system (400-500°C). The carbon dioxide fugacity of the Vesuvius hydrothermal system might be controlled by thermo-metamorphic reactions.

the vapour phase is close to 14.9 wt.% NaCl (1 m), whereas its maximum salinity is 49.2 to 52.5 wt.% NaCl (2m and 3m), corresponding to saturation with halite (Fig. 17).

As the salt contents of the aqueous solutions circulating in this system cannot be constrained satisfactorily, total fluid pressures (which are closely approximated by $PH_2O + PCO_2$) in the zones of the hydrothermal system where gases equilibrate, are also poorly constrained. They are 260 to 480 bar for vents FC2 and FC5 and 130 to 220 bar for vent FC1. Based on a simple hydrostatic model (Fig. 18), the hydrothermal reservoirs connected with these fumaroles are at depths of 2.6-4.8 km and 1.3-2.2 km, respectively. Consequently, the deepest hydrothermal reservoir appears to be within the carbonate sequence, which is at depths >2.5 km underneath the volcano, whereas the shallowest reservoir is in the overlying volcanic rocks.

Monitoring the thermodynamic conditions of this hydrothermal system trough the study of the fumaroles chemical composition is of primary relevance in the surveillance of Vesuvius.

A detailed CO_2 flux campaign on the Vesuvius cone, indicates that the degassing process of hydrothermal gases affects most of the slopes and bottom of the crater, and few spots on the slopes of the cone. A total CO_2 output is estimated at 100±20 td^{-1}.

Discussion points. - Transition from lava fountaining conditions to buoyant column reflects different fragmentation conditions in the conduit or modifications of the vent geometry? Non vesiculated juvenile material characterises the lithic dominated Vulcanian deposits suggesting that ground-water entered the conduit, and fragmentation was triggered by magma-water interaction. Hydrothermalised lavas and dykes are subordinate in the deposit suggesting a minor role of hydrothermal fluids in triggering Vulcanian explosions.

Stop 1.2:

The Osservatorio Vesuviano

Significance. The Osservatorio Vesuviano historical building, presently an information centre on volcanic hazards and risk.

The Osservatorio Vesuviano. - The Osservatorio Vesuviano, the oldest volcano observatory in the world, was founded in 1841 by king Ferdinand II of Bourbon. It was inaugurated during the 7th Congress of the Italian Scientists, held in Naples in 1845.

The historical building of the Osservatorio Vesuviano, the elegant work of the architect Gaetano Fazzini, is on the Colle del Salvatore at an elevation of 609 m a.s.l., between Ercolano and Torre del Greco. The position chosen was particularly favourable since the site, hosting already a small church and a hermitage dating back to 1600, had never been damaged by the very frequent eruptions, occurred after the large 1631 event. The first director was Macedonio Melloni, one of the most prominent experimental physicists. The construction was completed in 1848; only a few months later, for political reasons, Macedonio Melloni was dismissed as director. His successor was the physicist Luigi Palmieri, at the time professor of philosophy at the University of Naples, who provided the Osservatorio with a meteorological tower. Luigi Palmieri built the first electromagnetic seismograph, with which he wanted to "make the smallest motions of the ground clear, recording them on the paper or indicating their nature, strength and duration". He first detected harmonic tremor caused by magma oscillation and degassing in the conduit and concluded that such a phenomenon could be used to forecast an eruption. The following directors were Raffaele Vittorio Matteucci and Giuseppe Mercalli. The latter, inventor of the homonymous scale of seismic intensity, drew the first modern classification of volcanic eruptions. Ciro Chistoni and Alessandro Malladra followed Mercalli as directors . In 1937 Giuseppe Imbò was appointed as director. He strengthened the existing instruments on the volcano reaffirming the old objectives of Melloni and Palmieri on forecasting eruptions. He made instruments for seismological, electrical and radioactive observations, hoping to forecast the final eruption of the cycle begun in 1913. Imbò with the aid of a seismograph and observations on the Vesuvius activity, managed to forecast the 1944 eruption and to inform the authorities. He was director until 1970, the year of the first ascending phase of the recent Phlegraean bradyseismic events. In the second half of the 1990s the Osservatorio Vesuviano has gone through the most significant change of its long history. It was transformed into a volcano observatory capable of carrying out research and technical activities aimed at performing long- and short-term forecasting of volcanic eruptions, volcanic hazard assessment and zoning of the territory exposed to the hazards. In such an atmosphere, the historical building of the Osservatorio Vesuviano was transformed in a volcanology museum, with the aim of disseminating information on volcanic hazards and risk. At present the Osservatorio Vesuviano is a section of the Istituto Nazionale di Geofisica e Vulcanologia.

Discussion points. – Volcanic eruption forecasting. Information and education as tools for risk mitigation.

Stop 1.3:

The AD 79 eruption at Herculaneum excavations

Significance. – The most famous Plinian eruption and its effects on land and urban settlements.

The AD 79 "Pompeii" eruption. - On August 24 of AD 79, Vesuvius awakened, and destroyed the towns of Herculaneum, Oplontis, Pompeii and Stabiae. The eruption has been studied by many authors (Lirer et al., 1973; Sigurdsson et al., 1985; Barberi et al., 1989; Cioni et al., 1999; Gurioli et al., 2002) and three major phases have been distinguished: (1) opening phreatomagmatic; (2) main Plinian; (3) caldera-forming with phreatomagmatic surges and flow emplacement. Significant variations of the characteristics of the pyroclastic deposits have allowed the definition of Eruption Units, deposits emplaced by pulses within a phase, with well defined eruptive mechanism. The AD 79 eruption sequence includes 8 Eruption Units, each with distinct areal distribution and lateral variations (Fig. 19, 20).

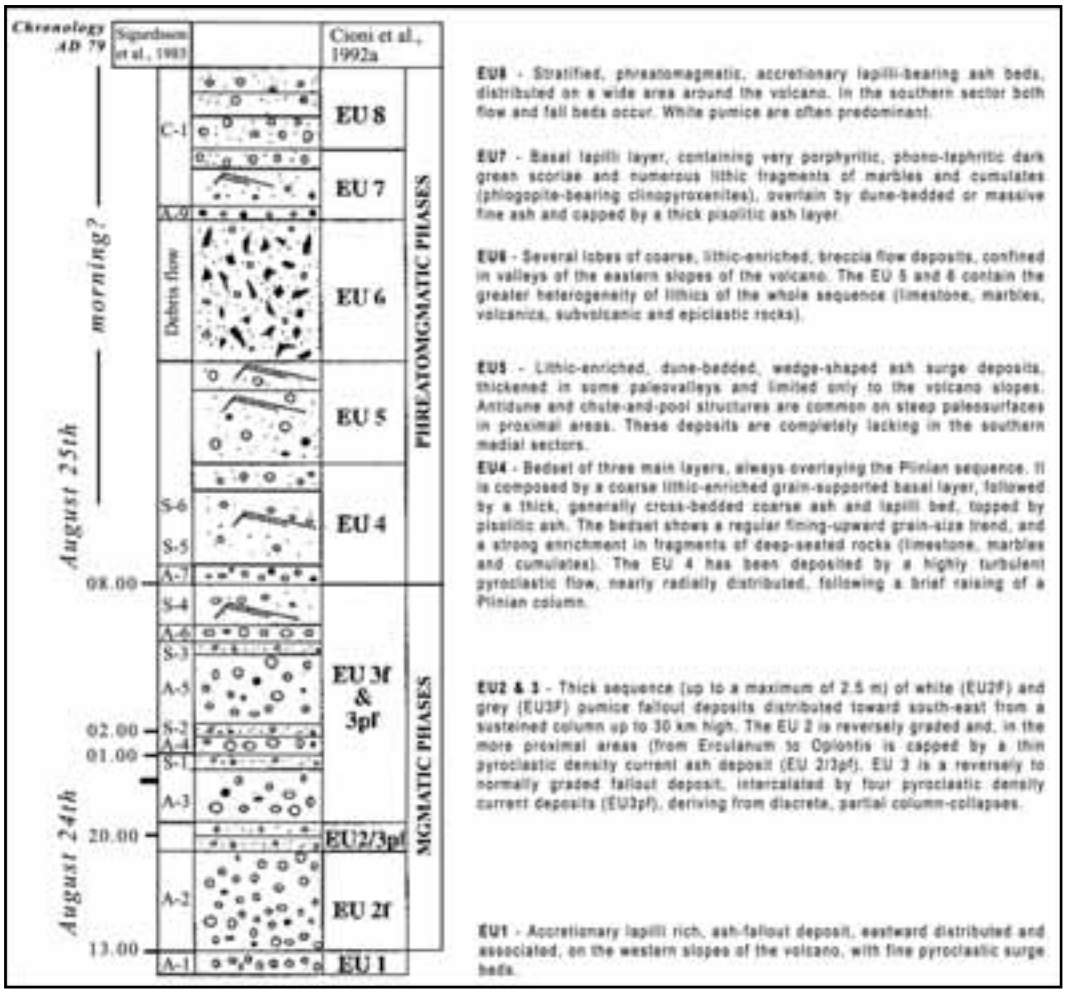

Figure 19 - Generalised sequence of the AD 79 Vesuvius eruption deposits.

An accretionary lapilli-rich ash layer (EU1), the only product of the opening phreatomagmatic phase, is covered by the pumice-fall deposit of the Plinian phase. This latter phase was dominated by an eruption column which reached a maximum altitude of 30 km. The Plinian deposit is composed of white phonolitic pumice ($EU2_F$), locally capped by a thin, whitish ash-flow deposit ($EU2/3_{PF}$), which passes upwards, with a sharp colour change, to grey, mafic phonolitic pumice ($EU3_F$). The upper part of the deposit contains intercalated ash-flow beds ($EU3_{PF}$) and is closed by pumice and ash flow deposits in proximal exposures. During this phase, which tapped more than 3 km^3 of magma, thick fallout deposits accumulated on a large area to the southeast, and pyroclastic-current deposits buried Herculaneum to the south. The caldera forming phase began with the most powerful and widespread pyroclastic current (EU4). The strong earthquake and the dark cloud witnessed by Pliny the Younger at Cape Misenum on the morning of August 25th is likely to correspond to this pyroclastic current. The currents of this phase destroyed human settlements along the western and northern slopes of the volcano and devastated the Pompei-Stabia area. The caldera-forming phase continued with the emplacement of the pyroclastic-current deposits of EU5, distributed in proximal areas and confined in valleys of the volcanic edifice. EU5 is covered by very coarse, lithic breccia flow deposits of EU6, extensively exposed along the eastern slopes of Mt. Somma.

Areal distribution as well as lithic types and content

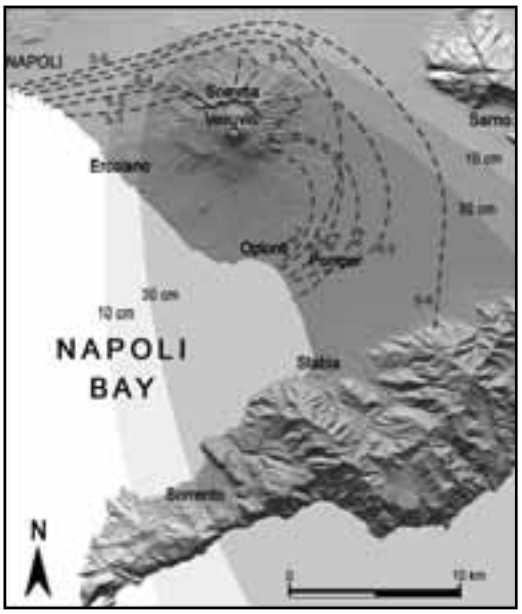

Figure 20 - Distribution of the AD 79 Vesuvius eruption deposits.

of the latter deposits, suggest that they were erupted during the paroxistic events of the caldera-forming phase. The protracted withdrawal of the magma chamber, favoured by magma-water interaction, led to tapping of the more mafic liquid that characterises the juvenile fraction of the widespread EU7. During the waning stage of the eruption, wet, phreatomagmatic, ashy pyroclastic currents (EU8) were generated, showing a sharp compositional reversal towards the more salic compositions of the initial phase of the eruption.

The Plinian deposits (fall and minor flows) range from early phonolitic white pumice to late tephritic-phonolitic grey pumice; the upper phreatomagmatic flow units exhibit larger variations with both grey and white pumice clasts and more abundant mafic crystals in the grey pumice. White pumice results from the withdrawal of phonolitic magma from the top of the chamber. Temperature was evaluated at about 850-900° on the basis of homogenisation temperature of glass inclusions in sanidine and leucite. The grey pumice results from the mixing of three isotopically distinct components: phonolitic white melt, mafic cumulates and a crystal-poor grey magma. The grey magma had high temperature (around 1050° C), very low viscosity and density slightly higher than that of the white magma. These features are consistent with the establishment of a physical discontinuity separating the white from the grey body. The lower portion of the Pompeii chamber was therefore occupied by a homogeneous, phonolitic-tephritic, grey magma which was never erupted without being largely mixed. The grey-white mixing was mainly sin-eruptive, as suggested by variations in magma discharge rate closely linked to the extent of the mixing.

The Herculaneum excavations

Herculaneum Beach. - The grey wall (23 m thick) including at least six units, is the best exposure of the AD 79 pyroclastic-current deposits that buried Herculaneum (Fig. 21).

These deposits lie on the old coastline. Along the waterfront a series of arches form the base of the Sacred Area. Each arch forms a chamber. On the southern part of the waterfront are the Suburban Thermae. The beach and the shoreline consisted of yellow tuff of the Avellino eruption, covered by black sand. The tuff formed a wave-cut platform whose surface was worked to provide a slip-way for large boats.

The first deposit of the eruption is a 35 to 50 cm thick unconsolidated, poorly sorted, massive grey surge layer (EU2/3pf) which extends into the chambers.

Figure 21 - The pyroclastic-currents deposits of the AD 79 Vesuvius eruption at the Herculaneum coast-line.

Volume n° 2 - from B16 to B33

All the skeletons of the human victims, as well as the skeleton of a horse, occur within this surge layer.
This unit overlies filling material, probably related to the restorations of the earthquake damages preceding the eruption, and is overlain by a lithified, pyroclastic lensoid pumice-flow deposit (EU3pf1). A 8 m long boat, was found in the first pyroclastic flow on the beach. The sequence follows with a fines-depleted, coarse grained, pumice rich layer (up to 200 cm thick) with abundant building material (EU3pf2a), cropping out on the downwind side of buildings, and thinning and fining away from the walls. This layer grades in the overlying massive, consolidated pumice flow deposit (EU3pf2b), <5 m thick, that thins towards the suburban Thermae, maintaining a horizontal upper surface. A fines-poor, discontinuous bed of pumice lapilli and lithic fragments (skarn, marbles and cumulitic rocks) represents the most important discontinuity visible in this area. Its scalloped bottom is clearly related to the deformation effect of ballistic blocks. This bed marks the transition to the thick (up to 15 m) lithic rich flow deposits of the phreatomagmatic phase, correlatable to the basal layer of EU4 in the southern sector of the volcano (EU4). A massive, consolidated pyroclastic flow (s) deposit (yellow tuff), 8 m thick, follows. The last deposit (F4) is a massive, poorly lithified, lithic rich pyroclastic flow, up to 5 m thick.

Palestra. Palestra is a rectangular park surrounded by porticos, and used for gymnastics, sports and games; in the centre of the park is a cross-shaped, 1.2 m deep swimming pool. It is covered by the EU3pf2 and EU4 deposits.
EU2/3pf includes a basal massive unit with a high amount of building material and a stratified upper part. Inside the Bourbon tunnels, it thickens locally up to 1.5 m. Inside the Palestra, EU3pf1 forms lenses, EU3pf2 directly overlies EU2/3pf, and shows a basal fines-poor layer, rich in building debris. EU3pf2 is overlain by EU4 and lithic rich pyroclastic deposits, 7 m thick.

DAY 2

Stop 2.1:

Traianello Quarry: the past 19,000 years of Somma-Vesuvius activity

<u>*Significance.*</u> – A long period of Somma-Vesuvius eruptive history is testified by the products exposed in the quarry. Occurrence of both fall and flow deposits of the Plinian events suggests a scarce control by the topographic barrier of the Mt. Somma caldera wall on their dispersion.

Figure 22 - General view of the Traianello quarry.

<u>*The quarry.*</u> - Traianello quarry (Fig. 22) is on the Mt. Somma slopes, 2 km north of Somma Vesuviana. In a small excavation within the quarry floor a 100-150 cm-thick brownish to reddish scoria deposit is exposed, this is related to eccentrical vents of Mt. Somma. In other parts of the quarry thin lava flows are interbedded with the scoria deposits.

The "Pomici di Base" tephra overlies the scoria bed. It is a compositionally zoned Plinian pumice-fall deposit, composed of a white pumice lower bed, surmounted by a grey banded and a black pumice beds. The upper part of the sequence, a stratified, lithic-rich fall layer surmounted by a dark ash-flow deposit, with sparse lithic and juvenile clasts, records the final phase of the eruption, dominated by phreatomagmatic explosions.
The "Greenish Pumice" Tephra mostly includes fall deposits with contrasting grain-size.
A layer of pedogenised yellowish ash, separates the "Greenish Pumice" Tephra from the Agnano Pomici Principali. The products of this Phlegraean eruption are widely dispersed over the Mt. Somma slopes and constitute an important marker bed.
The "Mercato Pumice" Tephra is well exposed in the central part of the quarry, along a 30 m high scarp. From base upwards it includes a white pumice-fall deposit, interbedded with a layer of pinkish ash, overlain by a thick sequence of pyroclastic-flow

Figure 23 - View from Camaldoli towards the east-southeast.

deposits. The pinkish ash that laterally passes to a pumice flow, with a very sharp lateral transition from faintly laminated to a massive pyroclastic flow. The upper pyroclastic-flow sequence includes several flow units, locally cross-stratified and characterised by a variable content of lithic blocks and juvenile clasts."
The "Avellino Pumice" Tephra partially fills palaeo-valleys. The Plinian fall deposit is characterised by a sharp change in colour from white at the bottom to grey at the top, reflecting a compositional change. An accretionary lapilli-rich ash layer and an overlying massive ash-flow deposit are at the top of the sequence, on the Plinian fall deposits, and are related to variable phreatomagmatic activity. The first can be correlated with a very impressive pyroclastic surge deposit outcropping in the western and north-western part of the volcano, while the second is linked to a less energetic, Vulcanian-type activity that formed an alternance of lithic-rich fall layers and pyroclastic flows, well exposed on the north-western slopes.
The AD 79 eruption, represented by at least four massive ash-flow units with abundant lithic blocks, close the stratigraphic sequence, filling the paleo-valleys partially occupied by the Avellino products.

Discussion points. - Pyroclastic flows of the Plinian eruptions of Somma-Vesuvius: lateral transitions and topographic influence. The effects of a caldera wall on the dispersal of pyroclastic currents.

Stop 2.2:

The Campi Flegrei caldera from the Camaldoli hill

Significance. - A general view of the active portion of the Campi Flegrei caldera.
The caldera. - From south counterclockwise, the island of Capri, the Sorrento peninsula, the Somma-Vesuvius, the city of Naples, the Campi Flegrei caldera, the islands of Procida and Ischia (Figs. 1, 2, 23).
The Sorrento peninsula and the island of Capri are part of the Apennine chain, intersected by NE-SW and NW-SE trending faults, which determine a horst-and-graben type structural pattern. The graben-type structure in the central part of the peninsula is partially filled by the Campanian Ignimbrite, on which is built the town of Sorrento.
A very good view of the Somma-Vesuvius and its relationships with the city of Naples and surrounding towns can be appreciated.The town of San Sebastiano is also well visible and the 1944 lava flow which destroyed it.
The Vomero-Arenella saddle was a preferential pathway for pyroclastic currents erupted in the Soccavo plain during the I epoch (15÷9.5 ka) of the third period of activity of the Campi Flegrei caldera.
The largest part of the morphological boundaries of both Campanian Ignimbrite and Neapolitan Yellow Tuff calderas, are visible. Towards the east, at Casalesio, the horizontally laying Campanian Ignimbrite is cut by a southward dipping high-angle surface, which is part of the Campanian Ignimbrite caldera margin overlain by the Neapolitan Yellow Tuff. The same relationships occur along an ENE-WSW alignment up to Poggioreale, towards the east, and up to Punta Marmolite, towards north-west.

The St. Martino hill is a complex morphology including a lava dome buried by a sequence of pyroclastic-surge deposits, all generated between the Campanian Ignimbrite and the Neapolitan Yellow Tuff eruptions. The scarp bordering the Posillipo hill towards the northwest, is the only exposed part of the Neapolitan Yellow Tuff caldera margin. The densely urbanized Fuorigrotta-Bagnoli and Soccavo plains, have been the site of eruption vents during the I epoch (15 - 9.5 ka) of the third period of activity.

Figure 24 - The Astroni crater from Camaldoli.

Looking towards the south-west, one can have a view of the almost complete caldera, and of the islands of Procida and Ischia. In the foreground the Agnano plain and the Astroni tuff ring. The former results from a volcano-tectonic collapse during the Agnano-Monte Spina eruption (4.1 ka) which will be discussed at Stop 3.1. Behind the Astroni and Gauro volcanoes, is the Averno-Capo Miseno alignment of tuff cones and tuff rings, which marks the western margin of the Neapolitan Yellow Tuff caldera. All these volcanoes but Fondi di Baia (8.6 ka), formed during the I epoch (15 ÷ 9.5 ka) of the third period of activity of the caldera.
The Astroni volcano, a well preserved elliptical edifice with axes of about 2 and 1 km, (Fig. 24), formed during the III epoch of activity (4.8-3.8 ka) of the Campi Flegrei caldera (Di Vito et al., 1999).

Isaia et al. (2004), on the basis of a stratigraphic study, have defined 7 depositional units, delimited by either thin paleosols or erosional unconformities.
The eruption vents, although confined in the present crater, migrated from NW to SE.
The volcano grew at the north-western edge of the Agnano-Monte Spina volcano-tectonic collapse, (4.1 ka), in the final part of the 4.1-3.8 ka time span. This implies that the 7 eruptions followed each other at very short time intervals. This conclusion is also supported by constancy in archaeological facies of findings within the paleosols between variable Astroni units, in the plain north of the caldera. The sequence of close eruptions makes the Astroni volcano peculiar in the recent history of the caldera. Therefore, the definition of its history is very important in order to understand one of the past phenomenologies of the caldera, and are relevant elements for forecasting its behaviour.

<u>Discussion points.</u> - Campanian Ignimbrite and Neapolitan Yellow Tuff calderas. Volcanism within the Neapolitan Yellow Tuff caldera. Volcanic hazard and risk of a megacity inside an active caldera.

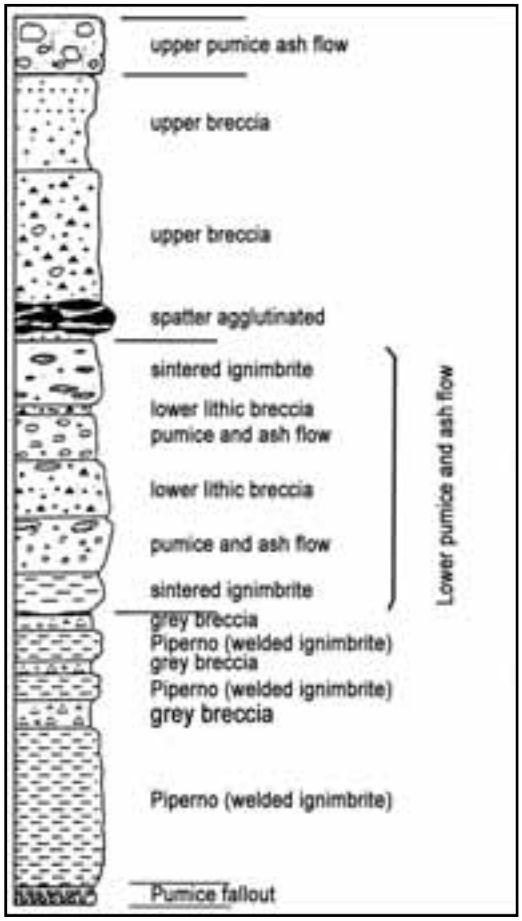

Figure 25 - Generalised eruption sequence of the proximal Campanian Ignimbrite (modified after Rosi et al., 1996).

Stop 2.3:

Verdolino quarry

<u>Significance.</u> - The caldera forming eruptions. Geometrical relationships among Campanian Ignimbrite, Neapolitan Yellow Tuff and interposed deposits.

<u>The Campanian Ignimbrite.</u> - The Campanian Ignimbrite catastrophic eruption occurred in the Phlegraean area and was accompanied by a caldera collapse (Rosi et al., 1999; Orsi et al., 1996; Ort et al., 2003; Pappalardo et al., 2002; Polacci et al., 2003). The collapsed area, about 230 km^2 (Fig. 6), includes the present Phlegraean Fields, the city of Naples, the bay of Pozzuoli and the north-western sector of the

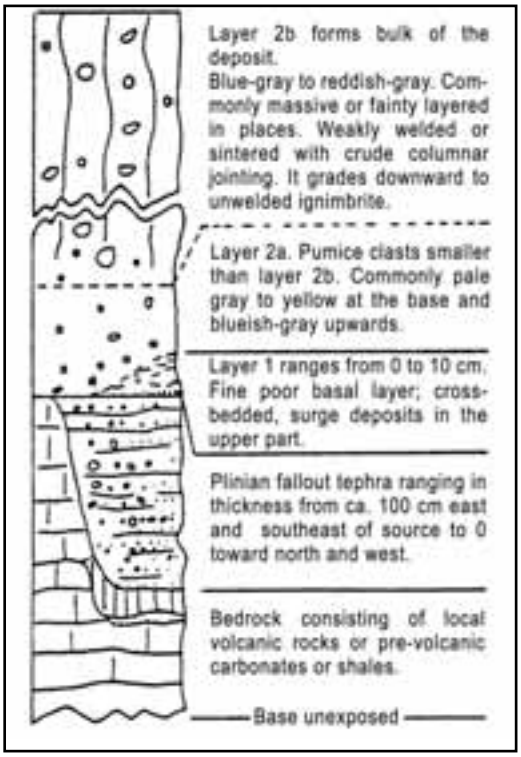

Figure 26 - Generalised eruption sequence of the distal Campanian Ignimbrite (After Fisher et al., 1993).

bay of Naples (Orsi et al., 1996).
The Campanian Ignimbrite sequence includes a basal Plinian fallout deposit surmounted by pyroclastic-current units, which in proximal areas are intercalated by densely welded ignimbrite (Piperno) and lithic-rich breccia units (Museum Breccia) (Fig. 25). The basal Plinian deposit (Rosi et al.,1999, Polacci et al., 2003), dispersed towards the east, consists of a well sorted and reversely graded lower portion, followed by a well to poorly sorted and crudely stratified upper portion. The pyroclastic-current deposits, which covered an area of about 30,000 km^2, show homogeneous sedimentological characteristics in medial and distal areas (10 to 80 km from the source) (Fisher et al., 1993).

From the base upwards, they include a very thin, discontinuous, fines-poor layer, above which lies the bulk of the ignimbrite (Fig. 26). They are partially welded to non-welded (greyish), although they can be lithified by zeolites (yellowish). These deposits, which underlie much of the Campanian Plain, also occur in isolated valleys in the Apennines, in the area of the Roccamonfina Volcano, and in the Sorrento Peninsula.
A stratigraphic and compositional study of a core drilled in the city of Naples, which includes four superposed pyroclastic-current units, has given to Pappalardo et al. (2002a) a unique opportunity to define the compositional features of the magma chamber, the timing of magma extraction, the withdrawal dynamics and the timing of the caldera collapse.

Pumice fragments range in composition from trachyte to phonolitic trachyte. Their phenocryst content decreases from the least evolved (10 vol%) to the most evolved (<3 vol%) samples. Phenocrysts are alkali-feldspar with subordinate plagioclase, diopside and salite clinopyroxene, biotite, magnetite and apatite. The stratigraphically uppermost Unit 4 contains the less evolved trachytic pumice, while the basal Units 1 and 2 contain the most evolved, alkali-trachytic to phonolitic fragments. Pumice fragments of Unit 3 have intermediate chemical composition. Major elements composition of glass from pumice fragments has a bimodal distribution. CaO content shows two modes, which correspond to the composition of the most and least evolved rocks, respectively. The composition of the glass from pumice fragments of Unit 3 comprises both modes. The geochemical variation detected in the cored units matches well those of the distal rocks, proximal breccia deposits and basal fallout beds (Pappalardo et al., 2002a and references therein). The degree of evolution of the erupted magma increased during the Plinian phase and decreased during the pyroclastic-current phase. The least evolved composition has been detected in the latest erupted magma and in glass inclusions hosted in clinopyroxene from the lower portion of the basal fallout deposit. Variation in major and trace element concentrations and constancy of Sr, Nd, Pb and B isotopic ratios, suggest that the eruption was fed by a trachytic magma chamber which included two co-genetic magma layers separated by a compositional gap (Pappalardo et al., 2002a). The upper layer was more evolved and homogeneous, whereas the lower layer was less evolved and zoned. During the course of the eruption, the two magma layers were extruded either individually or simultaneously producing the hybrid magma detected in Unit 3 of the core.
The eruption probably began with phreatomagmatic explosions, followed by the formation of a sustained Plinian column, which reached a maximum height

of about 44 km (Rosi et al., 1999) and was fed by simultaneous extraction of the two magma layers present into the chamber. Due to upward migration of the fragmentation surface, reduction of magma eruption rate, and/or formation of fractures, an unstable pulsating column was formed and fed only by the most evolved magma. The maximum height reached by this column was of about 40 km (Rosi et al., 1999).

This Plinian phase was followed by the beginning of the caldera collapse and the generation of expanding and initially over-pressurized pyroclastic currents fed by the upper magma layer. The currents moving northward, surmounted the Roccamonfina Volcano (>1,000 m a.s.l.) at 50 km from the source, while the southward currents reached the Sorrento Peninsula, over seawater. During the following major caldera collapse, the maximum mass discharge rate was reached and both magma layers were contemporaneously tapped as the intermediate composition magma, generating further expanding pyroclastic currents which travelled radially from the vent and deposited ignimbrites at distances in excess of 80 km. Towards the end of the eruption, only deeper and less differentiated magma was tapped, producing less expanded and less mobile pyroclastic currents, which travelled short distances within the Campanian Plain without crossing the Apennines or reaching the Sorrento Peninsula.

Figure 28 - Geographic distribution of the Campanian Ignimbrite deposits.

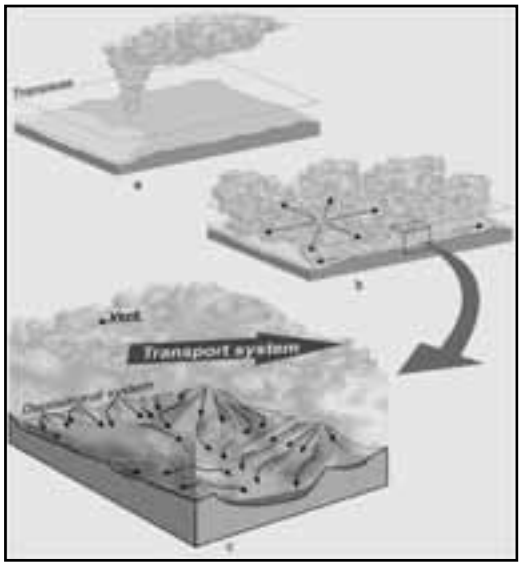

Figure 27 - The Campanian Ignimbrite eruption: main phases (a, b) and model of the transport and depositional systems of the pyroclastic currents (c) (After Fedele et al., 2003).

Fisher et al. (1993) and Ort et al. (2003) suggested that the pyroclastic currents which surmounted high mountain ranges and travelled over seawater were characterised by distinct transport and deposition systems (Fig. 27). Initial pyroclastic currents were expanding gas-particle mixtures that moved over the landscape as dilute currents. The transport system moved outward from source and was thicker than the highest relief. It was kept turbulent by the significant surface roughness. As the currents travelled away from the vent, they stratified continuously with respect to density, forming the deposition system in their lower part. This system, blocked by morphological obstacles and decoupled from the transport system, drained off ridges and down valleys in directions dictated by slope direction.

Ash layers related to the Campanian Ignimbrite eruption are known from cores in the Mediterranean Sea. The Y5 ash layer recognized from the Ionian Sea to the eastern Mediterranean and correlated with an oxygen isotope date of ca. 38,000 yr bp (Thunnel et al., 1979) has the same composition of the most evolved and intermediate Campanian Ignimbrite erupted magmas. Campanian Ignimbrite ash layers were also rec-

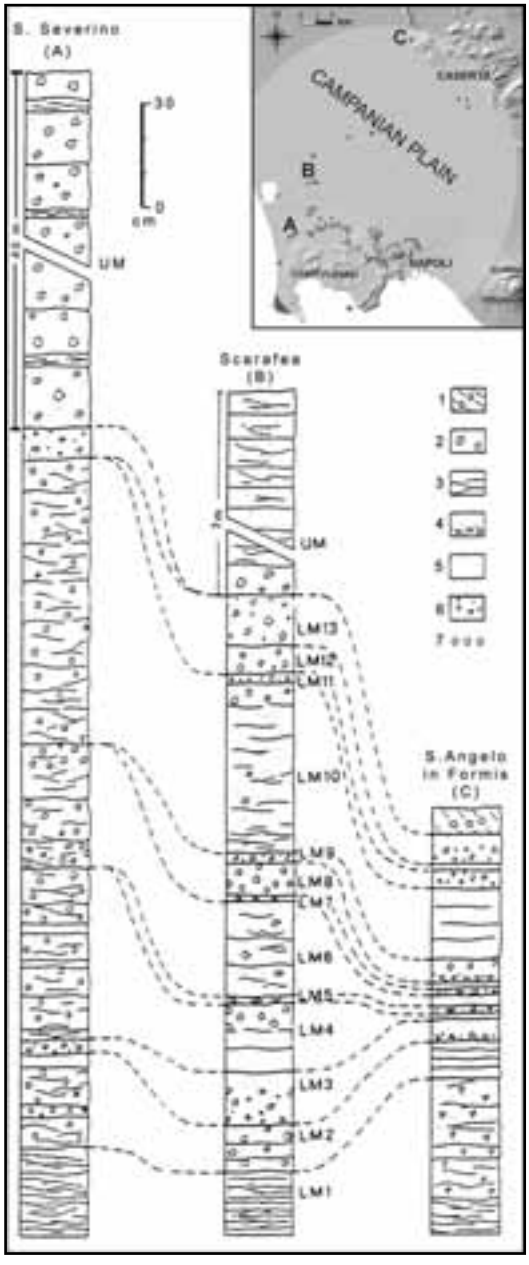

Figure 29 - Outcrop area and stratigraphic sections of the proximal (St. Severino), intermediate (Scarafea), and distal (Sant'Angelo in Formis) facies of the Neapolitan Yellow Tuff. 1: reworked deposits; 2: pyroclastic flow deposits; 3: pyroclastic surge deposits; 4: pumice-and-ash fallout deposits; 5: ash fallout deposits; 6: debris flow; and 7: accretionary lapilli. (after Orsi et al., 1992)

ognized in Greece (Seymour and Christanis, 1995) as well as in northern and central Italy, Bulgaria, and the former USSR (Narcisi and Vezzoli, 1999 and references therein) (Fig. 28). Fedele et al. (2004) estimated that the co-ignimbrite ash cloud rose in the atmosphere at a height of at least 30 km, and suggested that the ash layer could result from particle deposition within either the umbrella cloud of the Plinian columns or the transport system, of the pyroclastic currents. The latter, likely controlled by wind both at low altitude (<10 km) and in the stratosphere, laid down particles over a very large area. Furthermore, considering the sequence of phenomena, the characteristics of the pyroclastic currents, and the volume estimates for the variable portions of the eruption, the authors suggested that the erupted magma was >200 km^3 (DRE).

Fedele et al. (2004) evidenced the occurrence of the eruption during a time interval characterised by bio-cultural modifications in western Eurasia, including the Middle to Upper Palaeolithic transition and the supposed change from Neanderthal to "modern" Homo sapiens anatomy, a subject of continuing investigation and controversy. At several archaeological sites of south-eastern Europe, the ash separates the cultural layers containing Middle Palaeolithic and/or "Earliest Upper Palaeolithic" assemblages from those with Upper Palaeolithic industries. At the same sites the tephra coincides with a long interruption of occupation. The palaeoclimatic records show that the eruption occurred just at the beginning of Heinrich Event 4 (HE4), characterised by extreme climatic conditions, compared to the other HEs. The authors hypothesised a positive climate-volcanism feedback triggered by the co-occurrence of the eruption and HE4 onset.

The Neapolitan Yellow Tuff. - The Neapolitan Yellow Tuff is the second largest pyroclastic deposit of the Campanian area. Conservative estimates of the area covered by the tuff and volume of erupted magma are 1,000 km^2 (Fig. 29) and about 40 km^3 (DRE), respectively. The deposit, generally grey and poorly lithified in distal areas, in the proximal Neapolitan-Phlegraean area is zeolitised and yellow, from which the name. The tuff has attracted the interest of many geologists since the 19th century. Orsi et al. (1992; 1995) and Wohletz et al. (1995) reconstructed in details its stratigraphic and chemo-stratigraphic sequence, the eruption mechanisms, the feeding magmatic system, and the relationships among eruption dynamics, magma

withdrawal, and timing of caldera collapse. Orsi et al. (1996), reconstructed the structural boundary of the area collapsed during the eruption (Fig. 6).

The Neapolitan Yellow Tuff sequence was divided into a Lower Member (LM) and an Upper Member (UM) (Fig. 29), on the basis of textural characteristics, dispersal and occurrence of an angular unconformity. LM is the product of the largest known trachytic phreato-Plinian eruption. Its thickness varies from 11 m in the most proximal exposures, to 85 cm at Sant'Angelo in Formis, at the foot of the Apennine mountains, 35 km from the vent area. In contrast, the characteristics of UM are typical of a phreatomagmatic eruption. Its thickness varies from about 100 m in the Quarto Plain, to 7 m at Scarafea, in the Caserta Plain (Fig. 29).

LM includes 13 layers, designated LM1 through LM13 from base upward. Layer LM1 occurs over the entire outcrop area and is composed of many ash to coarse ash, millimetres to centimetres thick, surge beds; lapilli-sized components occur only in proximal areas. Often it shows cross laminations and erodes the underlying paleosol. Layers LM2, LM4, LM6, LM8, LM10 and LM12 include variable beds, composed of ash with high amount of accretionary lapilli, and few scattered pumice and hornfelsed lithic clasts. The beds vary from undulating and cross laminated to massive and plane-parallel with distance from vent, suggesting that in proximal area they were deposited dominantly by erosive surge clouds while in distal areas deposition was mostly due to ash fallout. Layers LM3, LM5, LM7, LM9, Lm11 and LM13 are pumice- and ash-fallout beds.

The basal pumice fallout contains a significant amount of ash and variable amount of lithic clasts. Size of pumice and lithic fragments not always decreases with distance from the vent. The upper ash fallout contains millimetre-sized pumice fragments and a large amount of accretionary lapilli.

UM is a sequence of pyroclastic-flow and -surge deposits which shows considerable variation with both distance from the vent and azimuth around the caldera. Pyroclastic-flow deposits dominate within the caldera, while pyroclastic-surge beds are the most abundant outside the caldera. Likely UM was generated by multiple fracture vent eruptions and pyroclastic currents were transformed (Fisher, 1983) across the caldera scarps.

The Neapolitan Yellow Tuff composition varies from latite to alkali trachyte. Phenocrysts (<3% by volume) are sanidine, plagioclase, clinopyroxene, biotite,

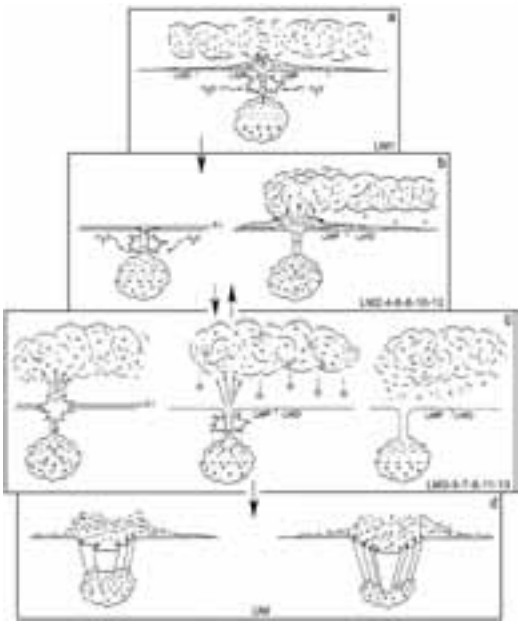

Figure 30 - Illustration of magma chamber withdrawal and eruption column behaviour during the Neapolitan Yellow Tuff eruption. The three magma types in the chamber are: alkali trachyte (dashes), trachyte (dots), and trachyte to latite (x) (after Wohletz et al., 1995).

magnetite, in order of decreasing abundance, and rare apatite. Sanidine in latite, anorthitic plagioclase in trachyte and alkali trachyte, reversely zoned plagioclase and two clinopyroxenes (diopside and salite) are evidence of mineralogical disequilibrium.

Compositional variation of pumice fragments, allows a fourfold distinction of the sequence, from the base upward in: LM alkali trachyte (LMat), LM trachyte (LMt), UM alkali trachyte (UMat) and UM alkalitrachyte-to-latite (UMt). Glass shards from the trachytic pumice-and-ash fallout beds of LM, show all the chemical compositions displayed by the pumice fragments of the whole sequence. Trace element, K_2O, Na_2O, SiO_2 and P_2O_5 contents distinguish the two trachytic groups, whereas the two alkali trachytic groups are distinguished by their stratigraphic position. LMat pumice has a fairly homogeneous composition. LMt pumice becomes progressively less differentiated up-section. LMt and LMat pumice are separated by a compositional gap. A compositional gap separates UMat from the underlying LMt. Umt includes alkalitrachytic to latitic pumice progressively less differentiated upsection, without any compositional gap with the underlying UMat. The stratigraphically lowermost

alkali trachytic sample of this group, enriched in Sr, Ba, K_2O and P_2O_5 and depleted in Na_2O, Zr, Nb, Th, REE with respect to the underlying UMat, marks the arrival of a new magma in the chamber. Pumice clasts from the least differentiated UMt sample, have latitic (dark) and trachytic (white) compositions, suggesting magma mingling, probably during extrusion.
The magma chamber was composed of three discrete layers: an upper alkali trachyte (magma 1), an intermediate trachyte (magma 2) and a lower alkali trachyte to latite (magma 3), separated by compositional gaps (Orsi et al., 1995). The three magmas, characterised by similar Sr-isotope ratio, are not related to crystal fractionation processes, and represent distinct magma batches originated from a similar deep source. Syneruptive mingling is documented by the occurrence of glass shards of variable composition in the same bed. The eruption was likely to have been triggered by the arrival of magma 3 into the chamber, and began (Fig. 30a) with explosions driven by efficient water/magma interaction that produced LM1. These explosions were fed by the uppermost, compositionally evolved, volatile- and likely bubble-rich, LMat layer of magma. After LM1, the character of the explosions abruptly changed.

The vesiculated LMt magma interacted with water and fragmented very efficiently, producing highly energetic phreato-Plinian explosions which generated LM2 (Fig. 30b). These explosions apparently flushed the water out of the conduit so that the following rising magma, which generated LM3, did not encounter a significant amount of water until it reached the sea floor. Only the upper part of this magma interacted efficiently with the sea water and was disrupted in fine particles, while the lower part was mainly fragmented by exsolution of the magmatic gases. Alternation of phreato-Plinian (LM2, LM4, LM6, LM8, LM10, LM12) and mostly magmatic (LM3, LM5, LM7, LM9, LM11, LM13) explosions was repeated six times after eruption of LM1. The phreato-Plinian explosions gave rise to surge emplacement in proximal areas and ash fallout in both proximal and distal areas. Accretionary lapilli were abundant due to a high amount of steam. In contrast, phreato-Plinian to magmatic explosions (Fig. 30c) generated sustained columns that dispersed downwind plumes of pumice laden with fine ash and steam experiencing premature ash fallout and formation of accretionary lapilli. Each phreato-Plinian explosion tapped all three magma layers, whereas the phreato-Plinian to magmatic explosions only drained the intermediate trachytic layer. Increase in withdrawal depth, evidenced by commingling of the three layers of the chamber, could result from a dramatic pressure decrease on the magma in correspondence of the conduit and/or from a large increase in eruptive mass flux, both consequences of the water/magma interaction efficiency during phreato-Plinian explosions.
A time break occurred after LM eruptions, and then activity resumed with very different characteristics in UM explosions (Fig. 30d). The time break is marked by initiation of a caldera collapse and a change from central-vent to ring-fracture eruptions. This change in vent character caused an overall pressure decrease on the chamber that allowed the previously trapped magma in the chamber top (UMat) to be erupted. The eruption then continued with the extraction of the deepest magma in the chamber (UMt). Water/magma interaction during UM eruptive phases was not as efficient as during LM phases. Explosions fed pyroclastic flows and surges. The caldera likely continued to collapse also after the end of the eruption, as suggested by the absence of any outcrop of Neapolitan Yellow Tuff in the central part of the Phlegraean Fields.
Wohletz et al. (1995) attempted to evaluate the physical parameters of the eruption. Calculations based on magma chemistry show an increase in magma density, a decrease followed by an increase in viscosity, and a general decrease of gas fraction during both LM and UM eruptive phases. From a depth of 400 m, calculated fragmentation depths gradually rise during each phase. Application of sequential fragmentation/transport analysis to granulometric data shows an average ratio of phreatomagmatic to magmatic components of 70:30 for LM and 80:20 for UM. However, computed water/magma interaction ratios generally decrease from about 0.65 to 0.05 and are fairly constant at about 0.1 during eruption of LM and UM, respectively. Furthermore, surge/flow run-out distances and estimates of eruptive velocities from R values show that column collapse heights were extremely high (6 to 7 km) during the first phase and were substantially lower during the second phase (2 to 3 km). Vent radii required for calculated eruption velocities of 180 to 370 m/s are between 70 and 300 m, suggesting a cumulative eruption duration of over 10 hours, perhaps spanning of one to several days.

The quarry. - In an old quarry dug at the mouth of the Verdolino valley, in the Soccavo plain (Figs. 6, 31), the oldest exposed rocks are Piperno and Breccia

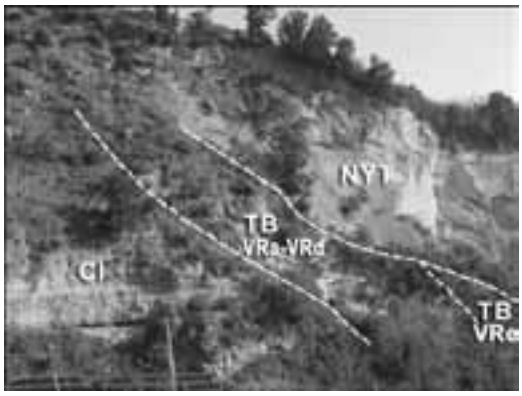

Figure 31 - View of the Verdolino valley from the south-west. CI: Campanian Ignimbrite; TB: Tufi Biancastri; VRa-e as in figure 32; NYT: Neapolitan Yellow Tuff.

Museo deposits of the Campanian Ignimbrite. They are overlain by pyroclastic deposits, named Tufi Biancastri (Whitish Tuffs), whose stratigraphic sequence, reconstructed by Orsi et al. (1996), is reported in figure 32.

Units VRa, VRb and VRd were generated by eruptions dominated by phreatomagmatic explosions

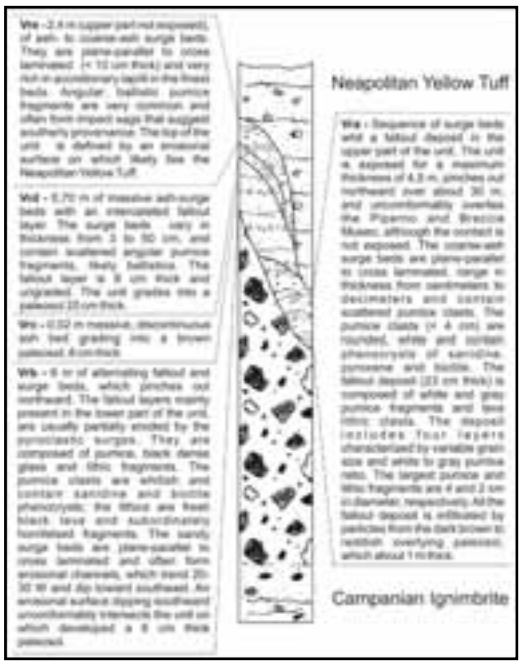

Figure 32 - Verdolino quarry stratigraphic sequence (after Orsi et al., 1996).

with minor magmatic events from vents located not far from the outcrop area. Unit VRc is a very thin and discontinuous ash bed. Unit VRe is the proximal deposit of a phreatomagmatic eruption whose vent was to the south of the Verdolino valley. The stratigraphically highest unit is the Neapolitan Yellow Tuff, which is deeply zeolitized throughout the area.
The sequence of Piperno and Breccia Museo, whose top is at about 200 m a.s.l., dips of about 6° towards the north and is intersected by an erosional surface dipping about 35° southward. Units VRa and VRb unconformably mantle this surface and die out toward its upper part. Both units are cut by an erosional surface, which dips about 30° southward and is mantled by Units VRc, VRd and VRe. All the exposed sequence up to unit VRe, is crosscut by a third erosional surface whose dip increases southward. This surface is mantled by the Neapolitan Yellow Tuff, whose thickness of about 100 m increases towards the Soccavo plain and whose base, at about 240 m a.s.l. at the top of the surface, is 170 m a.s.l. at its foot.

The erosional surface between Units VRb and VRc was likely to have been generated by an intense erosion during the Würmian sea level low stand (17-14 ka).

Discussion points. - Implications of deposit attitude and their geometrical relationships on caldera collapse features and morphological evolution.

DAY 3

Stop 3.1:

Pianura, Torciolano natural section - The Agnano-Monte Spina eruption

Significance. - Agnano-Monte Spina Tephra, the deposit of the highest magnitude eruption of the Campi Flegrei caldera in the past 5 ka.

The Agnano-Monte Spina eruption. - The Agnano-Monte Spina eruption history, including geometry and timing of the accompanying volcano-tectonic collapse, has been recently reconstructed by de Vita et al. (1999). The authors have also constrained its age to 4,100±50 y using ^{14}C (AMS) and $^{40}Ar/^{39}Ar$ methods. Variation of lithological features and occurrence of a well-defined erosional unconformity were used by the authors to subdivide the whole sequence into six members named A through F, which represent as many eruption phases. Details for each member are reported in figure 33. Dellino et al. (2001; 2004a),

Figure 33 - Agnano-Monte Spina Tephra type section (after de Vita et al., 1999).

Volume n° 2 - from B16 to B33

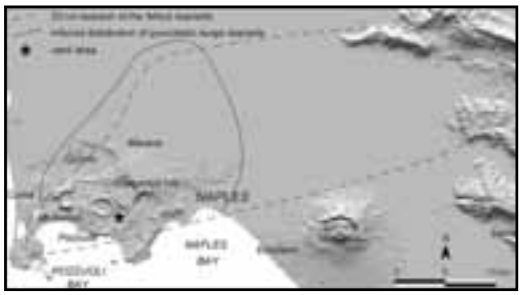

Figure 34 - Distribution of the Agnano-Monte Spina Tephra.

have discriminated the role of variable fragmentation dynamics operating in each eruption phase. The sequence alternates pyroclastic-current and -fallout beds, distributed over an area of about 1,000 km^2. The fallout beds are dispersed towards the north-east (Fig. 34). High particle concentration pyroclastic currents were confined in the Agnano depression, while lower concentration currents overtopped the morphological boundary of the caldera and travelled at least 20 km over the surrounding plain. Thickness of the tephra varies from a maximum estimated value of about 70 m in the Agnano plain, the inferred vent area for the eruption, to a few centimetres over a distance of about 50 km. Analysis of lateral facies variations and vertical facies associations of correlated layers reveals that during some eruption phases (layers B2, D2 and E2) the contrasting eruptive dynamics were almost contemporaneous (Dellino et al., 2004a). The phreatomagmatic origin of the pyroclastic-current deposits, which contrasts with the magmatic origin of fallout beds, suggests that the pyroclastic density currents did not result from eruption column collapses. They were most likely related to radially spreading clouds which were contemporaneous with fallout activity but issued from distinct zones in the vent area. Turbulence and high expansion made the base surges capable, under certain conditions, of passing over high topographic obstacles, with hazardous effects in distal areas. Dellino et al. (2004b), using a physico-sedimentological model, reconstructed both velocity and density of pyroclastic currents of layer E2 and calculated a dynamic pressure of the flow of about 3.1 kPa.

The Agnano-Monte Spina Tephra range in composition from trachyte to alkali-trachyte. Pumice and scoria fragments are porphyritic, with phenocrysts of feldspar, clinopyroxene, black mica, apatite and opaques in order of decreasing abundance. Olivine is present only in few samples. Clinopyroxene generally is green salite, very rarely is diopside. Feldspar phenocrysts are both normally or reversely zoned bytownitic plagioclase and homogeneous sanidine. Black mica is a Mg-biotite, fluor-apatite often forms inclusions in Mg-biotite and salite crystals, and opaque is a Ti-magnetite.

Pumice clasts of the lower portion of the stratigraphic sequence are more evolved (alkali-trachyte), those of the upper portion are less evolved (trachyte), whereas those of the middle part of the sequence have intermediate composition. Furthermore, beds with texturally and chemically variable pumice fragments also occur in the middle portion of the sequence. Sr-isotope ratio in the alkali-trachyte is about 0.70748, while for trachyte it ranges from 0.70750 to 0.70756. The alkali-trachyte of the lower portion of the stratigraphic sequence contains mineral phases in isotopic equilibrium. Conversely the trachyte of the upper portion shows isotopic disequilibrium among whole-rock and some mineral phases.
The isotopical and geochemical data suggest the existence of a stratified reservoir containing two isotopically distinct magma layers. The upper layer was slightly less-radiogenic and alkali-trachytic, while the lower layer was more-radiogenic and trachytic in composition. The two layers partially mixed during the course of the eruption. The occurrence of xenocrysts of olivine, An-reach plagioclase and Mg-reach clinopyroxene suggests that also a mafic magma might have been involved in the eruption. The detected Sr-isotope range is similar to that of the Neapolitan Yellow Tuff suggesting that the magma which fed the eruption could be differentiated residues of the Neapolitan Yellow Tuff magmas still present into the Phlegraean system.
The Agnano-Monte Spina is the highest-magnitude eruption occurred over the past 5.0 ka years within the Campi Flegrei caldera. A volume of magma of about 2.4 km^3 (D.R.E.) was extruded through a vent located in the sector of the resurgent after, affected by NW-SE fault systems related to an extensional stress regime (Orsi et al., 1996).
The eruption began with explosions driven by efficient water/magma interaction and generation of a highly expanded ash cloud which deposited the thin and widely dispersed basal part of layer A1. As a consequence of these explosions, water was driven out of the conduit, and the next explosion was magmatic and

generated a relatively low (about 5 km) column, which deposited the upper fall-out bed of layer A1. Phreatomagmatic and magmatic explosions, generated the pyroclastic-surge and -fallout deposits of layer A2. During this phase the upper alkali-trachytic batch of magma was tapped. The second phase began with magmatic explosions generating a pulsating column which reached a maximum eight of about 23 km and deposited the fallout layer B1. The basal beds of layer B2 were deposited by pyroclastic currents, generated by explosions which tapped the upper alkali-trachytic batch of magma. At this stage a network of fractures, foreshadowing a volcano-tectonic collapse, likely formed and became the site of scattered vents. Opening of fractures allowed ground water to access variable parts of the reservoir. Therefore, the following explosions were triggered by variable magma-water interaction efficiency and produced pyroclastic surges and Strombolian fallout. Fragmentation surface deepened and tapped a magma resulting from mingling between the alkali-trachytic and the trachytic magma batches. Such a mingling was likely favoured by pressure lowering on the reservoir. A pause in the eruption, and heavy rains caused diffuse erosion along steep slopes. Magmatic fine ash settled down, also favoured by rain flushing, to form Member C. Increase in fracturing of the roof rocks caused a lowering of the lithostatic pressure on the reservoir, at this stage containing only the trachytic magma batch. Pressure lowering determined volatiles exsolution in the trachytic magma and its migration towards surface. This rising magma interacted with the geothermal system, causing its flashing. The following phreatomagmatic explosions marked the renewal of the eruption and the beginning of the third phase with deposition of the D0 base surge deposits. Again the pressure wave drove the water out of the conduit. The following explosions were magmatic and generated an eruption column about 27 km high, that deposited layer D1. Activation of faults along the margins of the present Agnano plain produced the main episode in the volcano-tectonic collapse. The collapsed area, corresponding to the present Agnano Plain, has a polygonal shape and is bordered by NW-SE and NE-SW trending high-angle scarps (Fig 35). These rectilinear features, many of which include triangular facets, were generated by the activation of new faults and partial re-activation of pre-existing faults.

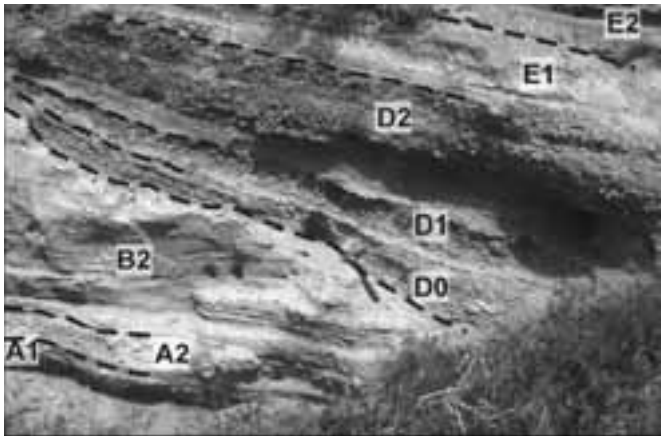

Figure 36 - The Agnano-Monte Spina Tephra at Torciolano.

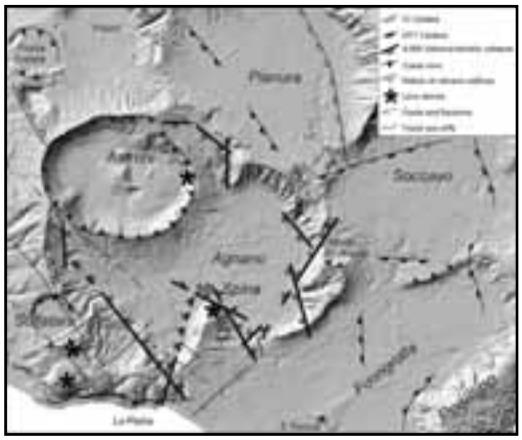

Figure 35 - Structural map of the Agnano plain.

The collapsed area is about 6 km^2 and the collapse was about 60 m, on average. Related to this collapse pyroclastic currents were generated within the caldera depression (layer D2). New vents opened along the faults and erupted pyroclastic surges that overtopped the northern sector of the morphological boundary of the caldera and flowed into the plain. Variation of the structural setting of the Agnano area allowed a large amount of ground water and geothermal fluids to access the reservoir. The following phreatomagmatic explosions marked the beginning of the fourth phase of the eruption, during which highly expanded ash cloud were erupted through vents along the structural boundary of the volcano-tectonic collapse. During the fifth and last phase of the eruption, magma supply

was discontinuous and progressively decreasing. A series of discrete phreatomagmatic explosions generated the ash beds of Member F. Settling of particles suspended in the atmosphere, likely favoured by rainfall, marked the end of the eruption.

The Torciolano exposure. - A sequence of the Agnano Monte Spina Tephra is exposed along the north-eastern side of the relict of the Pisani volcano, between Pianura plain and Camaldoli hill (Fig. 35). The exposure is a typical sequence of this tephra at intermediate distance from the vent area (Fig. 36).
Discussion points. - Magmatic vs phreatomagmatic explosions. Lithological and petrological evidences for volcano-tectonic collapse. A Plinian eruption in a densely populated area.

Figure 37 - The Solfatara crater.

Stop 3.2:

The Solfatara volcano

Significance. - A low-magnitude explosive eruption of the Campi Flegrei caldera in the past 5.0 ka. Crater geometry versus structural lineaments. Geochemical monitoring of active volcanoes.
The volcano. - The Solfatara volcano (Fig. 37), about 2 km east-northeast of Pozzuoli, is characterised by a sub-rectangular (0.5x0.6 km) crater, shaped by NW-SE and SW-NE trending faults (Fig. 35).
The Solfatara Tephra (Di Vito et al., 1999) overlies the Monte Olibano and Accademia lavas, both younger than Agnano-Monte Spina Tephra (4.1 ka) and underlies the Astroni Tephras (3.8 ka), from which it is separated by a thin paleosol containing many charcoal fragments. It is distributed over a small area (<1 km^2), and comprises a phreatomagmatic coarse breccia overlain by a sequence of pyroclastic-surge deposits, alternating with pumiceous fallout beds. The breccia contains large blocks of green tuff, altered lavas and dark scoriaceous bombs engulfed in an hydrothermally altered matrix. It is overlain by stratified, dune-bedded deposits composed of accretionary lapilli-bearing ash layers and thin, well-sorted, rounded pumiceous lapilli beds. The juvenile

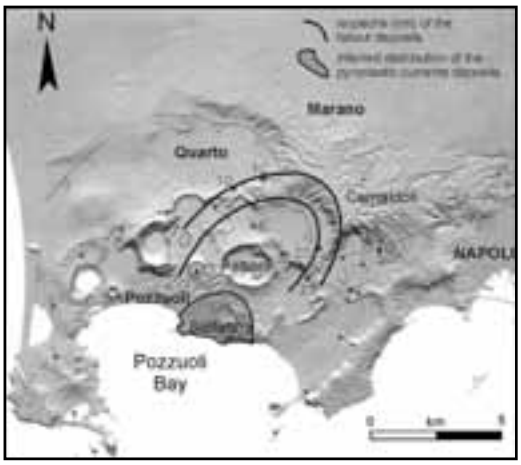

Figure 38 - Distribution of the Solfatara Tephra.

fragments are porphyritic scoriae (basal breccia) and crystal-poor to subaphyric pumice (upper sequence). The scoriae contain crystals of sanidine, plagioclase, clinopyroxene, biotite and Fe-Ti oxides, in order of decreasing abundance. Rare crystals of leucite converted to analcime are also present. The late erupted pumice fragments are alkalytrachytic in composition and contain rare crystals of plagioclase. A thin layer exposed at Cigliano, Torre Caracciolo and Verdolino is likely a distal counterpart of the Solfatara Tephra (Fig. 38) (Di Vito et al., 1999).
This layer, grey to yellowish in colour, is massive and consists of fine-to-coarse ash with scattered pumice clasts and interbedded pumice beds. It is a fallout deposit dispersed towards the north-east with a minimum measured thickness of 5 cm at Verdolino, about 7 km from vent. The sedimentological characteristics of the Solfatara Tephra suggest that the eruption was dominated by phreatomagmatic, with subordinate magmatic explosions.

The geothermal system. - The crater of the Solfatara has been the site of an intense hydrothermal activity

since Greek times. It is the most impressive manifestation of the present hydrothermal activity of the caldera, which includes both focused vents, with a maximum temperature of about 160°C (Bocca Grande fumarole), and large areas of hot steaming ground. The average molar composition of the fluids is H2O about 82 %, CO2 17.5%, H2S 0.13% and minor amounts of N2, H2, CH4 and CO. The isotopic compositions of H2O, CO2 and He suggests the involvement of magmatic gases in the feeding system of the fumaroles (Chiodini et al., 1997). Subsequently the original magmatic gases are condensed by an aquifer system as suggested by the absence of the soluble acid gases SO2, HCl and HF, typical of the high-temperature volcanic gas emissions. Boiling of this heated aquifer(s) generates the Solfatara fumaroles.

At present the Solfatara is the main object of the geochemical surveillance of the caldera. In particular both the chemical compositions of the fumarolic fluids and CO2 fluxes from the soil of the crater are monitored.

The hydrothermal system can be simplified in three main zones:

zone 1) - a heat source represented by a relatively shallow (few kilometres deep) magma chamber;

zone 2) - an aquifer located above the magma chamber. The magma body transfers to the aquifer(s) mainly heat, causing an intense boiling process;

zone 3) - the shallower part of the system is characterised by the presence of superheated vapour produced by boiling of the aquifer. In 1982, temperature and pressure, estimated on the base of gas composition, were close to the conditions of maximum enthalpy of the steam (236°C, 31 bar).

Since the 1982 unrest, systematic geochemical monitoring began providing 175 samples (from 1983 to 2003) for the hottest vent (Bocca Grande, T = 150–164°C), that is considered representative of the entire fumarolic field of Solfatara. Strong variations involving both main and minor gas species were observed during the bradyseismic crises in 1982–1984, 1989, 1994, and 2000. A physical modelling was recently applied to explain these recent bradyseismic crises (Chiodini et al., 2003). The model hypothesizes periodic injections of hot CO2-rich fluids at the base of a shallow hydrothermal system (Fig.1), consistent with the observed chemical variations. Moreover the model predicts an average increase in pore pressure and temperature within the system, suggesting potential effects on ground deformation. Interestingly, compositional peaks systematically follow the corresponding maximum uplift, with a delay of the order of few hundreds days (Fig. 39).

Systematic measurements of the soil CO2 fluxes from the Solfatara crater began in 1995. The measurements are done with the accumulation chamber 'time 0' method which allows one to perform quick and reliable punctual measurements (Carapezza and Granieri, 2004).

The evolution in time of the degassing process is monitored through the following 3 different types of measurements:

- detailed campaigns covering most of the floor of the Solfatara crater (4-5 per year). Soil CO_2 flux and soil temperature (20 cm depth) at 200 points regularly spaced, are measured during each campaign . Therefore three specific campaigns (400 measurement points), covering the entire anomalous area of the Solfatara, were carried out in March-April 1998, in July 2000 and in July 2003. The results are impressive: the area degas about 1000-1500 ton/d of CO_2. This amount is of the same order of magnitude or higher than the amount of gas released from an erupting volcano;

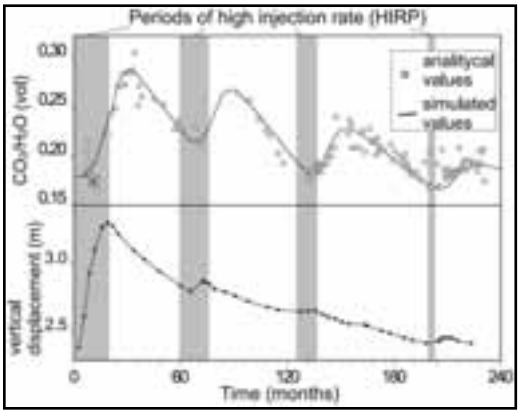

Figure 39 - (a) Comparison between observed (open dots) and simulated (solid line) gas composition expressed as CO_2/H_2O (molar ratio). The shaded area highlights periods of enhanced fluid injection (HIRP); (b) Ground deformation.

- quick campaigns (50-70 per year). Sixty selected, fixed, points are weekly measured in order to investigate the seasonal variations of the degassing process;
- continuous measurements. Since October 1997

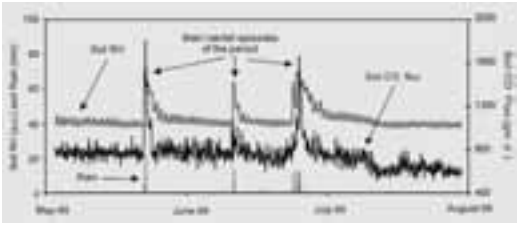

Figure 40 - Soil relative humidity, soil ϕCO2 and rainfall chronograms at Solfatara site from May to August, 1999. The positive anomalies of the soil humidity, due to rainfall episodes, produce a growth in the soil ϕCO2.

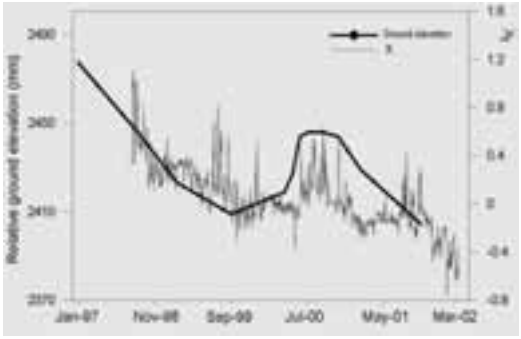

Figure 41 - Long-term trend of the filtered soil CO_2 signal (Xt) and soil deformation chronograms at Solfatara site. The best correlation is obtained by back-shifting the Xt series by three months.

an automatic station measures soil CO_2 fluxes and environmental parameters (air temperature, air humidity, air pressure, wind speed, soil temperature and soil humidity) (Fig. 40). The measurements are performed every 2 hours. The statistical analysis of dataset showed that (1) the highest frequency fluctuations are due to variations of environmental parameters (particularly soil humidity and air temperature) and (2) the long-term trend of the filtered data is correlated with the ground deformation (Granieri et al., 2003) (Fig. 41).

Discussion points. - A volcano in a fumarolic stage within a densely populated area. Does a low-magnitude explosive eruption generate hazards in urban areas?

Stop 3.3:

Averno lake

Significance. - Averno 1 and 2, and Mt. Nuovo eruptions, the only eruptions within the north-western sector of the Campi Flegrei caldera in the past 5 ka.

The volcano. - Averno 1 (4.5 ka), Averno 2 (3.7 ka)

Figure 42 - Stratigraphic sequence of the Averno 2 Tephra

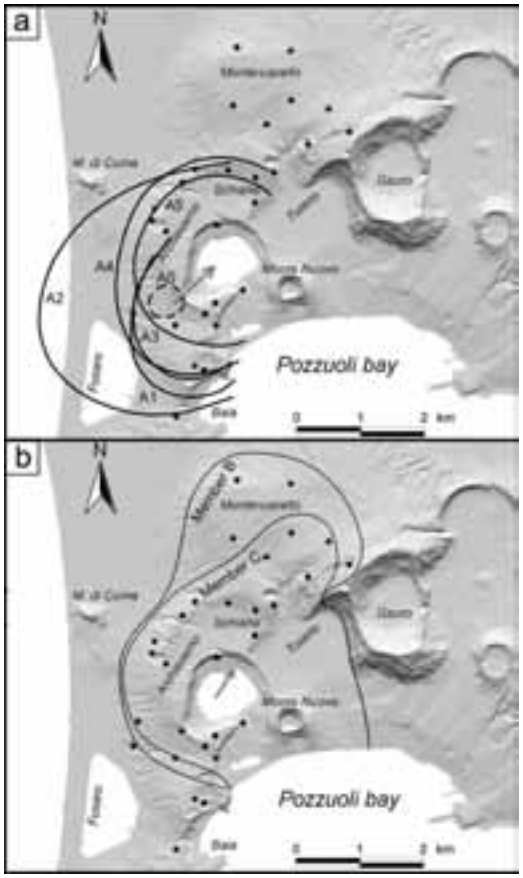

Figure 43 - Distribution of the Averno 2 Tephra. a: isopachs of the fallout deposits of Member A, arrow indicates direction of vent migration; b: pyroclastic-currents deposits of Member B and C.

and Mt. Nuovo (1538 AD) are the only three eruptions over the last 5 ka in the northwestern sector of the Campi Flegrei caldera, at the intersection of NE-SW and NW-SE fault systems, bordering towards the north-west the most uplifted portion of the resurgent block within the Neapolitan Yellow Tuff caldera floor (Orsi et al., 1996).

The Averno 2 eruption was characterised by magmatic and phreatomagmatic explosions which produced a sequence of pyroclastic-fall and -surge deposits. The whole sequence has been subdivided into three members named A through C (Fig. 42; Di Vito et al., 2004).
Member A was emplaced during the first phase of the eruption by prevailing magmatic explosions which generated six fallout beds deposited by columns reaching a maximum height of 10 km.
The subsequent phases of the eruption generated explosions driven by variably efficient water-magma interaction with formation of wet to dry surges, which emplaced Member B and C, respectively. Isopachs and isopleths maps of fallout deposits, as well as areal distribution of both ballistic fragments and facies of surge beds (Fig. 43), suggest a vent migration during the course of the eruption from south-west to north-east, likely along the NE-SW fault system. This migration contributed to the irregular shape of the crater, elongated towards the south-west, and presently filled by a perennial lake. The erupted magma was about 0.05 km^3 (DRE).

Pumice fragments show variable vesicularity and porphyricity. Texture varies from aphyric to porphyritic and glomero-porphyritic, with groundmass mostly holohyaline. Porphyricity ranges from less than 1 to about 9 vol. % of plagioclase, alkali-feldspar, biotite and clinopyroxene. The first erupted rocks are weakly peralkaline alkali-trachyte, while the last erupted are alkali-trachyte. Sr- and Nd-isotope ratios are constant throughout the sequence; slightly more radiogenic values have been detected in fallout layers 3 and 4 of Member A.
Variation of major and trace elements content suggests that during the eruption two distinct magma layers were tapped. The most evolved, peralkaline, uppermost magma layer was tapped during the first phase, while the least evolved, lowermost magma layer was extruded during both last magmatic phases of Member A, and last phreatomagmatic phases of the eruption. The slightly peralkaline character of the magma, as well as of those feeding the other eruptions occurred in the western sector of the Campi Flegrei caldera over the past 5 ka, suggests that only in this sector small batches of magmas can stagnate at shallow depth for a time long enough to drive their chemical character toward peralkalinity. Furthermore, a slight though significant change in the geochemical and isotopic characteristics of the products occurred during emplacement of Member A, contemporaneously with the first migration of the vent. Thus, the eruption demonstrates that a close relationship may exist between structural setting and magma composition and variation, even in a very small magmatic system.

<u>Discussion points.</u> – *The* relationships among deformation dynamics, eruption vents location and magma composition in a resurgent caldera.

Stop 3.4:

Serapeo Marketplace and bradyseismic events

Significance. - Short-term deformation in a resurgent caldera.

The Serapeo. - Ground deformation in the Neapolitan Yellow Tuff caldera over the past 2 ka, is documented at the Serapeo roman monument in Pozzuoli (Parascandola 1947). The Serapeo (Fig. 44), located few tens of meters inland at Pozzuoli, was first supposed to be a temple devoted to the Egyptian god Serapis, from which the name. Only at the beginning of last century was recognized as a marketplace. Excavation of the monument began in 1750, by order of Charles of Bourbon the king of Naples, in an area called "the vineyard of the three columns" because three marble columns were coming out of the ground. After excavation, the columns showed lythodomes holes up to 7 m above the floor of the monument, testifying the maximum subsidence of the area (Fig. 44).

Figure 44 - The Serapeo marketplace at Pozzuoli.

The monument, constructed between the end of the I and the beginning of the II century AD, was restored at the beginning of the III century AD because sea water had invaded its floor. Since then the ground was subsiding until the X century AD when it began to uplift (Fig. 6d). This uplift lasted until the 1538 Monte Nuovo eruption. Since the beginning of the XVI century AD there was an acceleration of the uplift as testified by royal edicts with which newly-formed land was ceded to the town of Pozzuoli. In the last few days before the Monte Nuovo eruption an uplift of 5 to 8 m took place in the vent area (Parascandola, 1947). After the eruption the ground has subsided until 1969 (Fig. 6d).

Issel (1883) coined the word bradyseism (from the greek bradi = slow and seism = movement) to mean slow subsidence or uplift of the ground. The word is in use in the volcanological literature on the Campi Flegrei caldera since the beginning of last century to mean the vertical ground movements in historical times.

Two major unrest episodes (bradyseismic events) have occurred between 1969 and 1972, and 1982 and 1984 (Fig. 6d) (see Orsi et al. 1999a for references). The maximum ground uplift was about 170 and 180 cm, respectively. Since 1984 the ground has been generally affected by subsidence interrupted by small episodes of inflation in 1989 (7 cm), 1994 (<1cm), and in 2000 (4 cm), with maximum ground deformation always in the area of Pozzuoli. Only 85 cm of the net uplift has been recovered.

Orsi et al. (1999a) performed detailed analyses of short-term ground deformation and seismicity of the 1982-84 unrest episode. The shape of the deformation despite its amount and versus, is invariant in time and space. Furthermore, the analysis of the vertical ground movement carried out along three alignments radially distributed around the area of maximum deforma-

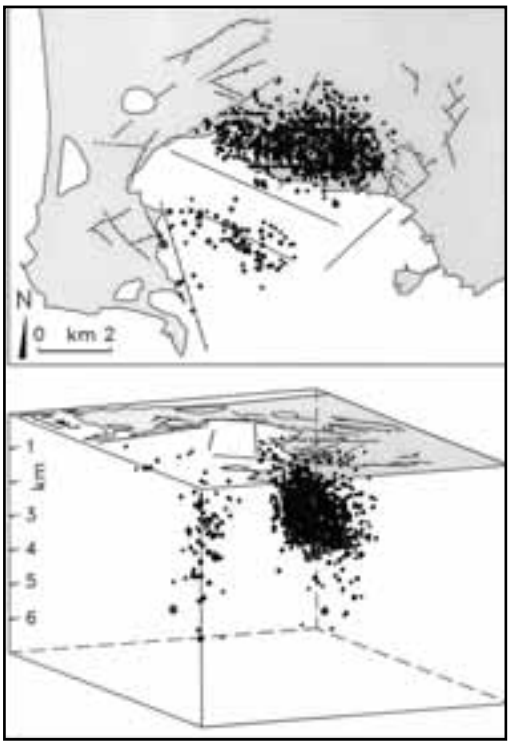

Figure 45 - Plan and 3D view from south-east of the hypocentres of earthquakes occurred in the 1982-84 unrest episode.

tion, showed significant breaks in slope, independent from amount and versus of the ground movement, in correspondence of known structural discontinuities. Seismicity was concentrated mostly in the area of the maximum vertical movement and subordinately in the western part of the bay of Pozzuoli. The depth of the hypocentres varied from a few meters to about 5 km (Fig. 45).

The hypocenters of the events occurred along the Averno-Capo Miseno and Mofete-Banco di Nisida alignments, span from very shallow depth to 5 km. Those of the events occurred along the faults systems bordering the seismogenetic area towards the north-west and the south-east, were at intermediate depth. Focal mechanisms showed four main solutions: normal, normal/strike-slip, strike-slip and reverse/strike slip. Most of the events occurred between the San Vito-Agnano alignment and the Pozzuoli coast showed normal-type solution. The events that occurred along the Mofete-Nisida alignment were characterised by reverse/strike-slip and strike-slip solutions.
This short-term deformation has been interpreted by Orsi et al. (1996, 1999a, c) as the result of the interplay of a ductile and a brittle component. The authors have suggested that both components are generated by a pressure and temperature increase in the shallow magma reservoir due to the arrival from depth of small magma batches, less evolved and hotter than the resident magma. The ductile component could result from the expansion and migration of geothermal fluids due to temperature increase. The brittle component could be generated by a slip along fault planes in the shallow crust above the magma reservoir. Ground deformation data and both epicentres and hypocentres location of the earthquakes occurred during the bradyseismic events and show that the deformed area has a polygonal shape defined by fault systems of the resurgent block inside the Neapolitan Yellow Tuff caldera (Orsi et al., 1999a). This geometry is also well constrained by SAR interferometry data (Lundgren et al. 2001). The striking similarity between ground deformation geometry occurred during the recent bradyseismic events and that of the III epoch, suggests that the resurgence dynamics is not changed since the quiescence period between the II and III epoch. The similarity in shape between long- and short-term deformation corroborates the hypothesis that the former results from the summation of many short-term deformation events (Orsi et al., 1996).

Discussion points. - Relationships between long- and short-term deformation in a resurgent caldera. Hazards related to unrest episodes. Relationships between unrest episodes and eruptions.

DAY 4

Stop 4.1:

Ischia

Significance. - A circumnavigation of the island, devoted to the illustration of its stratigraphical, volcanological, structural and geomorphological features.
From Ischia Porto to Carta Romana. - The Ischia harbour was made in 1853-54 by cutting a narrow strip of land, separating a crater lake from the sea (Fig. 46). The deposits related to this crater are

Figure 46 - The Ischia harbour crater: view from north.

alkalitrachytic scoria fallout layers and surge beds, which overlay a paleosol containing archaeological findings of the VI-V century BC (see Sansivero, 1999 for references).
Out of the harbour, the area comprised between Costa Sparaina and Mt. Rotaro is well exposed south-westward (Fig. 47). Costa del Lenzuolo is a half moon shaped ridge that degrades toward the morphological heights of Bosco dei Conti to the east. Its morphology results from lava domes covered by pyroclastic deposits younger than the XI century AC The morphological heights toward west are the Mt. Maschiata-Montagnone complex. The superimposition of the Montagnone dome (the northernmost height) over the remnant of the Mt. Maschiata dome is clearly visible (Fig. 47).
The pine-wood extending from the coast south-westward, grows on the lava flows of the 1302 AD Arso eruption (Fig. 47), the last on the island.. The flows, erupted from a vent located 2.7 km inland, have a maximum width of 1 km, a thickness of 40-50 m and vary in composition from trachyte to latite.

The islet on which the Aragonese Castle is built is an

Volume n° 2 - from B16 to B33

Figure 47 - View from NE of the area between C. Sparaina and Mt. Rotaro.

alkalitrachytic lava dome (130 ka). The northern cliff is a section through the central part of the dome along which its feeding conduit and internal structure are well exposed (Fig. 48).
Beyond the islet a well exposed steep scarp is the morphological evolution of a NE-SW trending regional fault that downthrown the northern part of the Mt. Vezzi block (Fig. 49). The rocks that compose this block, the oldest outcropping on the island, are exposed along the cliffs of the south-eastern coast. The flat lowland to the north-west of Mt. Vezzi is bordered toward west by a series of differentially displaced blocks, whose uplifting is maximum for the Mt. Epomeo. Most of the vents active in the past 10 ka are in this area, which is under an extensional stress regime due to the simple-shearing mechanism of resurgence.
At Carta Romana there are many subaqueous thermal springs whose alignment follows a regional tectonic trend.

Figure 48 - The northern slope of the Aragonese castle lava dome (130 ka).

<u>From Carta Romana to Punta della Signora.</u> - At the southern end of the Carta Romana beach, a sea cliff extends along the south-eastern coast up to Punta della Signora. From Carta Romana to II Porticello bay, the base of the cliff is composed of alkalitrachytic lavas of the Parata unit (73 ka). These lavas are overlain by pyroclastic-fall and -flow deposits belonging to variable units. Pyroclastic-fall deposits erupted either at Procida or at the Campi Flegrei caldera, occur in this sector of the island. They overlay products older than 75 ka. At Punta della Pisciazza, erosion has dissected a dome and a scoria cone (>75 ka), both alkalitrachytic. The feeding system of the dome is well exposed. The sea floor between the islands of

Figure 49 - View from NE of the Torone-Mt. Cotto alignment, bordering toward north a flat lowland.

Ischia and Procida is characterised by morphological features, likely remnants of volcanic cones.
A section through a trachybasaltic scoria cone and its feeding system is well exposed at Grotta di Terra (Fig. 50). The cone lies on a NE-SW trending fracture, parallel to the already described regional fault system. Its eruption marked the beginning of the 28-18 ka period of activity. The succession exposed in the sea cliff includes from top to bottom: pyroclastic deposits of the last period of activity (<10 ka); the scoria deposit and the feeding dyke of the Grotta di Terra cone (28

Figure 50 - Grotta di Terra. 1: lavas older than 75 ka; 2: pyroclastic deposits aged between 75 and 55 ka; 3: pyroclastic deposits of the 55-33 ka period of activity; 4: trachybasaltic Grotta di Terra dyke and scoriae (28 ka); 5: pyroclastic deposits of the past 10 ka.

ka); pyroclastic deposits of the 55-33 ka period of activity; pyroclastic deposits aged between 75 and 55 ka; lava flows older than 75 ka.
In the central part of the II Porticello bay, pyroclastic deposits overlay the Parata lavas, while in the western part, up to Punta della Cannuccia, they overlay lava flows of the Mt. Vezzi complex (126 ka). The oldest rocks on the island are exposed in this area, behind the Spiaggia di San Pancrazio. The San Pancrazio promontory is composed of a sequence of lavas of

Figure 51 - View of the eastern part of the Scarrupata di Barano cliff. 1: lava flows older than 75 ka; 2: pyroclastic deposits aged between 75 and 55 ka; 3: Mt. Epomeo Green Tuff sequence; 4: pyroclastic deposits of the 28-18 ka period of activity; 5: pyroclastic deposits of the past 10 ka.

the Mt. di Vezzi volcanic complex, intercalated with pyroclastic deposits. The upper part of this sequence includes the Mt. Epomeo Green Tuff.

The Scarrupata di Barano is a sea cliff that extends from Punta San Pancrazio to La Guardiola promontories (Fig. 51). Along this cliff the stratigraphic relationships among the products of the oldest activity are discernible, as they are little deformed by tectonics. The massive yellow-white ignimbrite, which forms most of the top of the cliff (marked at its base by a black scoria layer), has previously been correlated with the Mt. Epomeo Green Tuff. Work is currently being undertaken on the Mt. Epomeo Green Tuff stratigraphy and on earlier erupted deposits (Brown et al., 2004).

The La Guardiola, Capo Grosso and Punta della Signora promontories are composed of alkalitrachytic lavas (147 ka) overlain by this yellow-white ignimbrite and by later pyroclastic units, which are mainly composed of pyroclastic-fall and -flow deposits.

From Punta della Signora to S. Angelo promontory.

The Lido dei Maronti is a beach between Punta della Signora and S. Angelo promontories. At its eastern termination we will cross again the fault bordering the Mt. Vezzi block. Coastal exposures are the products of the dismantling of the Mt. Epomeo block, which are composed of very recent landslides and mud-flows, and older catastrophic debris avalanches that travelled as far as 40 km toward south (Chiocci et al., 1998). At the base of the S. Angelo promontory an alkalitrachytic lava dome (100 ka) is overlain by block-and-ash-flow and pyroclastic-fall and -flow deposits belonging to explosive volcanism that preceeded the Mt. Epomeo Green Tuff eruption (Brown et al., 2004). This is overlain by pyroclastic deposits aged between 55 and 20 ka. The youngest pyroclastic unit (20 ka), mostly composed of pyroclastic-surge deposits, lies unconformably over the older rocks. The S. Angelo village is built on mud flows that overlay these pyroclastic deposits.

From S. Angelo promontory to Punta Imperatore.

- The cliff between S. Angelo and Punta Chiarito is eroded into the surge deposits forming the top of the S. Angelo promontory.The Punta Chiarito promontory (Figs. 52, 53) is composed of alkalitrachytic lava flows, unconformably overlain by the youngest pyroclastic unit of the S. Angelo sequence. The uppermost deposits are the products of superficial gravitational movements.

In the bay between Punta Chiarito and Capo Negro, a NNE-SSW trending fault downthrows the eastern side bringing into contact the unit overlying the Punta Chiarito lavas with a pyroclastic sequence, likely of the 55-33 ka period of activity (Fig. 52).

The Capo Negro promontory is composed of alkali-

Figure 52 - View of the Chiarito bay. 1: lava domes older than 75 ka; 2: pyroclastic deposits of the 55-33 ka period of activity; 3a, 3b and 3c: pyroclastic deposits of the 28-18 ka period of activity.

Figure 53 - View between Capo Negro and P. Chiarito. 1: lava domes older than 75 ka; 2: pyroclastic deposits of the 55-33 ka period of activity; 3: pyroclastic sequence aged between 28 and 20 ka; 4: pyroclastic deposit aged at 20 ka

trachytic lava flows overlain by the same pyroclastic unit, which is in turn overlain by two thick pyroclastic units; the youngest of which is dated at 20 ka (Fig. 53).

The rocks exposed between Capo Negro and Punta Imperatore belong to the 28-18 ka period of activity.
The cliff between Capo Pilaro and Grotte del Mavone includes alkalitrachytic lavas with minor welded-scoria layers of the Pilaro complex, overlain by a sequence of alternating welded-scoriae and pumice-fall layers of the Scarrupo di Panza complex, and two younger pyroclastic units.

At the base of the Grotte del Mavone promontory, alkalitrachytic lavas (28 ka) are exposed.
In the cliff between Grotte del Mavone promontory and Punta Imperatore, a section through the Scarrupo di Panza volcano is well exposed. The section in its middle part is composed of a thick sequence (ca.100 m) of intensely welded scoriae, while at Grotte del Mavone, towards the south, and at Punta Imperatore, towards the north, it includes alternating layers of pumice-fall and welded scoriae interpreted by Rittmann (1930) as the products of a lava lake. In the bay between Grotte del Mavone and Punta dello Schiavo, this sequence is overlain by alkalitrachytic lavas (24 ka) and by two pyroclastic units composed of pyroclastic-fall and -surge deposits. Therefore the Scarrupo di Panza eruption must have occurred between 28 and 24 ka bp.
The base of Punta Imperatore promontory is composed of alkalitrachytic lavas (117 ka) covered by a pyroclastic breccia erupted prior to the Mt. Epomeo Green Tuff (Brown et al., 2004). This lithic breccia is overlain by a thick (c. 40 m) pumice-fall breccia with several intercalated scoria layers. A white ignimbrite, which may relate to the Mt. Epomeo Green Tuff eruption, fills a small valley cut into this thick fall deposit (Fig. 54). On the southern slope of the promontory this sequence attains a maximum thickness of 50 m and is unconformably covered by the products of the Scarrupo di Panza eruption that are in turn unconformably overlain by the pyroclastic units of the 28-18 ka period of activity. Along the northern side of the promontory, beneath the products of the Scarrupo di Panza eruption, is the Pietre Rosse pyroclastic unit (46 ka), which pinches out at the western end of the slope. This unit overlies the Mt. Epomeo Green Tuff and the sequence of pyroclastic units separated by paleosols that along this side of the promontory, pinches out eastward.
From Punta Imperatore to Zaro. –The Citara beach extends between Punta Imperatore and Pietre Rosse . Along the cliff behind the Citara beach, the Pietre Rosse unit is well exposed and contains

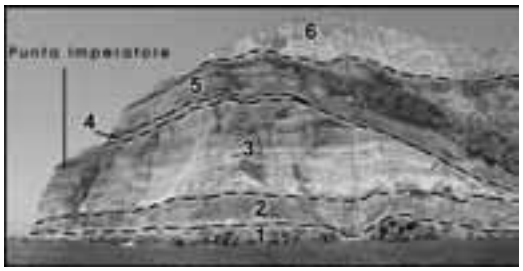

Figure 54 - Punta Imperatore promontory. 1: lava flows older than 75 ka; 2: breccia deposit at the base of the sequence aged between 75 and 55 ka; 3: pyroclastic sequence aged between 75 and 55 ka; 4: Mt. Epomeo Green Tuff sequence; 5: deposit of the Scarrupo di Panza volcano; 6: pyroclastic deposit of the 28-18 ka period of activity.

U-shaped channels. This tuff can be followed from Punta Imperatore to Pietre Rosse and represents the remnant of a tuff-ring whose vent was very likely located in this stretch of sea. A good section of this tuff is exposed at Pietre Rosse (Fig. 55). From its base upwards the sequence includes an ignimbrite deposit surmounted by a succession of surge beds with intercalated pumice-fall deposits.
From Pietre Rosse to Zaro the coast is low and formed by piles of landslide and debris-flow deposits derived from the Mt. Epomeo block. From this position it is possible to have a good view of the western slope of the Mt. Epomeo block (Fig. 56).
It is bordered by inward dipping, high angle reverse

Figure 55 - Pietre Rosse promontory. Natural section of the exposed pyroclastic sequence.

faults, whose directions vary from N40E to NS and N50W, from the north-western to the south-western parts of the block, testifying a compressional stress regime. These features are cut by late outward dipping normal faults due to gravitational readjustment of the slopes (Marotta, 2001). The north-eastern and south-western sides are bordered by vertical faults with right transtensive and left transpressive movements, respectively (Marotta, 2001).

Rione Bocca is the only locality within the resurgent area where the base of the Mt. Epomeo Green Tuff is exposed. Here, it overlies several metres of marine sediments, which in turn overlie an alkalitrachytic lava (133 ka). Recent work has shown that the Mt. Epomeo Green Tuff, as exposed at Rione Bocca, comprises two flow-units, each comprising a coarse heterolithic breccia at their base that passes up into a massive crystal and pumice rich ignimbrite (Brown et al, 2004). These flow units are separated by several metres of reworked, slumped and convoluted sediments. Towards Ciglio and Serrara the contact between yellowish pyroclastic deposits (33 ka) dipping at high angle south-westward, and the Mt. Epomeo Green Tuff is exposed. The contact is defined by a high-angle reverse fault generated by the Mt. Epomeo block resurgence. The high dip of the pyroclastic deposits is due to tilting produced by faulting. This geometrical relationships is an evidence that resurgence is active at least since 33 ka bp.

Sailing northward, beyond the Forio village there is the Zaro promontory, composed of a discrete number of superposed lava domes and flows, likely emplaced in a short time-span, along a complex network of N45E, N50W and subordinately E-W trending fractures. The vents for this volcanism are among the very few of the last period of activity located outside the eastern sector of the island.

Figure 56 - The western slope of Mt. Epomeo block between Ciglio and Capo dell'Uomo.

<u>*From Zaro to Ischia Porto.*</u> - Doubled the Zaro promontory we will find ourselves in the San Montano bay which is delimited by the Zaro lava domes and flows and the Mt. Vico promontory. The basal part of Mt. Vico promontory is composed of phonolitic lavas (75 ka). On these lavas, in small morphological depressions, is a sequence of pyroclastic-fall deposits of unknown provenance separated by paleosols. On the eastern slope of the Mt. Vico promontory, the lavas are unconformably covered by deposits attributed to the Mt. Epomeo Green Tuff that are in turn overlain by a succession of pyroclastic-surge and minor -fall beds (San Montano unit; 33 ka). On the upper part of the promontory, above a paleosol containing archaeological findings of roman age, is a pyroclastic deposit of uncertain provenance. Between Mt. Vico and Casamicciola the coast is cut into landslide and debris-flow deposits

Volume n° 2 - from B16 to B33

derived from the Mt. Epomeo block, whose northern slope is well visible. This slope is an E-W trending section through the block and shows its asymmetrical shape with the high angle western slope and the gently degrading eastern slope. From Casamicciola to Ischia Porto the products of the past 10 ka of activity are well exposed. They include lava flows and domes and both magmatic and phreatomagmatic pyroclastic deposits of the Mt. Rotaro and Mt. Montagnone composite volcanoes, older lava flows and domes and the remnant of some tuff-cones, aged between the XIII and the VIII century BC.

Discussion points. - Relationships among magmatism, tectonism, volcanism, volcano-tectonism and surface processes.

References cited

Arienzo, I., Civetta, L., D'antonio, M. and Tonarini, S. (2004). Mantle and crustal component for the genesis of phlegraean volcanic district. Earth Planet. Sci. Lett., submitted.

Arrighi, S., Principe, C. and Rosi, M. (2001). Violent Strombolian Eruptions at Vesuvius During post-1631 Activity. *Bull. Volcanol.* 63, 126-150.

Auger, E., Gasparini, P., Virieux, J. and Zollo, A. (2001). Seismic Evidence of an Extended Magmatic sill Under Mt. Vesuvius, *Science*, 9918.

Ayuso, R.A., De Vivo, B., Rolandi, G., Seal Ii, R.R. and Paone, A. (1998). Geochemical and isotopic (Nd-Pb-Sr-O) variations bearing on the genesis of volcanic rocks from Vesuvius, Italy. *J. Volcanol. Geotherm. Res.* 82, 53-78.

Barberi, F., Bizouard, H., Clocchiatti, R., Metrich, N., Santacroce, R. and Sbrana, A. (1981). The Somma-Vesuvio magma chamber: a petrological and volcanological approach. Bull. Volcanol. 44, 295-315.

Barberi, F., Cioni, R., Rosi, M., Santacroce, R., Sbrana, A. and Vecci, R. (1989). Magmatic and phreatomagmatic phases in explosive eruptions of Vesuvius as deduced by grain-size and compositional analysis of pyroclastic deposits. *J. Volcanol. Geotherm. Res.* 38, 287-307.

Belkin, H.E., De Vivo, B., Roedder, E. and Cortini, M. (1985). Fluid inclusion geobarometry from ejected Mt. Somma-Vesuvius nodules. *Am. Mineral.* 70, 288-303.

Bianco, F., Castellano, M., Milano, G., Ventura, G. and Vilardo, G. (1998). The Somma-Vesuvius stress field induced by regional tectonics: evidences by seismological and mesostructural data. *J. Volcanol. Geotherm. Res.* 82, 199-218.

Brancaccio, L., Cinque, A., Romano, P., Rosskopf, C., Russo, F., Santangelo, N. and Santo, A. (1991). Geomorphology and Neotectonic Evolution of a Sector of the Tyrrenian Flank of the Southern Apennines, (Region of Naples). *Z. Geomorph N. F.* 82, 47-58.

Brocchini, D., Principe, C., Castradori, D., Laurenzi, M.A. and Gorla, L., (2001). Quaternary evolution of the southern sector of the Campanian Plain and early Somma-Vesuvius activity: insights from the Trecase 1 well. *Mineral. Petrol.* 73, 67-91.

Brown, R. J., Orsi, G., de Vita, S. and Civetta, L. (2004). Multiple caldera collapse episodes on Ischia. in prep.

Buchner, G. (1986). Eruzioni vulcaniche e fenomeni vulcanotettonici di età preistorica e storica nell'isola d'Ischia. *In* «Tremblements de terre, eruptions volcaniques et vie des hommes dans la Campanie antique» (Centre Jean Bérard, Institut Français de Naples Ed.), 7, 145-188.

Carapezza, M.L and Granieri, D. (2004). CO_2 soil flux at Vulcano (Italy): comparison of active and passive methods and application to the identification of actively degassing structure. *Applied Geochemistry*, 19/1: 73-88..

Cecchetti, A., Marianelli, P. and Sbrana, A. (2001). A deep magma chamber beneath Campi Flegrei? Insights from melt inclusions. GNV Framework Program 2000-2002, I year results: 59-65.

Chiocci F.L., Sposato A., Martorelli E. e gruppo di ricerca TIVolI (1998). Prime immagini TOBI dei fondali del Tirreno centro-meridionale (settore orientale). Geologica Romana 34, 207-222.

Chiodini, G. and Marini, L., (1998). Hydrothermal gas equilibria: the H_2O-H_2-CO_2-CO-Ch_4 system. *Geochim. Cosmochim. Acta* 62, 2637-2687.

Chiodini, G., Frondini, F., Magro, G., Marini, L., Panichi, C., Raco, B., and Russo, M. (1997). Chemical and isotopic variations of Bocca Grande fumarole (Solfatara volcano, Phlegrean Fields). *Acta Vulcanologica* 8 (2), 228-232.

Chiodini, G., Marini, L. and Russo, M., (2001). Geochemical evidence for the existence of high-temperature hydrothermal brines at Vesuvio volcano, Italy. *Geochim. Cosmochim. Acta* 65 (13), 2129–2147.

Chiodini, G., Todesco, M., Caliro, S., Del Gaudio, C., Macedonio, G., and Russo, M. (2003). Magma degassing as a trigger of bradyseismic events: the case of Phlegrean Fields (Italy). *Geophys. Res. Lett.* 30, 1434.

Cioni, R., E. Corazza, and L. Marini, (1984). The

gas/steam ratio as indicator of heat transfer at the Solfatara fumaroles, Phlegrean Fields (Italy). *Bull.Volcanol*. 47, 295–302.

Cioni, R., Santacroce, R. and Sbrana, A. (1999). Pyroclastic Deposits as a Guide for Reconstructing the Multi-Stage Evolution of the Somma-Vesuvius Caldera. *Bull. Volcanol.* 60, 207-222.

Cioni, R., Sulpizio, R. and Garruccio, N. (2003). Variabilità of the eruption dynamics durino a Subplinian event: the Greenish pumice eruption of Somma-Vesuvius (Italy). *J. Volcanol. Geotherm. Res*. 124, 89-114.

Civetta, L. and Santacroce, R. (1992). Steady state magma supply in the last 3400 years of Vesuvius activity. *Acta Vulcanologica* 2, 147-159.

Civetta, L., D'Antonio, M., De Lorenzo, S., Di Renzo, V. and Gasparini, P. (2004). Thermal and geochemical constraints to the "deep" magmatic structure of Mt. Vesuvius. J. Volcanol. Geotherm. Res., in press.

Civetta, L., Gallo, G. and Orsi, G. (1991a). Sr- and Nd- isotope and trace-element constraints on the chemical evolution of the magmatic system of Ischia (Italy) in the last 55 ka. *J. Volcanol. Geotherm. Res.* 46, 213-230.

D'Antonio, M., Civetta, L., Arienzo, I., Carandente, A., Di Renzo, V., Di Vito, M.A., Giordano, F. and Orsi, G. (2004). Magmatic history of Mt. Vesuvius on the basis of new geochemical and isotopic data. *J. Petrol.,* in press.

D'Antonio, M., Civetta, L., Orsi, G., Pappalardo, L., Piochi, M., Carandente, A., de Vita, S., Di Vito, M. A., Isaia, R. and Southon, J. (1999). The present state of the magmatic system of the Campi Flegrei caldera based on the reconstruction of its behaviour in the past 12 ka. *J. Volcanol. Geotherm. Res.* 91, 247-268.

D'Argenio, B., Pescatore, T. S. and Scandone, P. (1973). Schema geologico dell'Appennino Meridionale. *Acc. Naz. Lincei, Quad*. 183, 49-72.

de Vita, S., Orsi, G., Civetta, L., Carandente, A., D'Antonio, M., Di Cesare, T., Di Vito, M.A., Fisher, R.V., Isaia, R., Marotta, E., Ort, M., Pappalardo, L., Piochi, M. and Southon, J. (1999). The Agnano-Monte Spina eruption (4.1 ka) in the resurgent, nested Campi Flegrei caldera (Italy). *J. Volcanol. Geotherm. Res.* 91, 269-301.

De Vivo, B., Rolandi, G., Gans, P.B., Calvert, A., Bohrson, W.A., Spera, F.J. and Belkin, H.E. (2001). New constraints on the pyroclastic eruptive history of the Campanian volcanic Plain (Italy). *Mineral. Petrol.* 73, 47-65.

Deino, A.L., Orsi, G., Piochi, M. and de Vita, S. (2004). The age of the Neapolitan Yellow Tuff caldera-forming eruption (Campi Flegrei caldera – Italy) assessed by $^{40}Ar/^{39}Ar$ dating method. *J. Volcanol. Geotherm. Res.,* in press.

Dellino, P., Isaia, R. and Veneruso, M. (2004b). Turbulent boundary layer shear flow as an approximation of pyroclastic surge: implication for hazard assessment at Phlegraean Fields. *J. Volcanol. Geotherm. Res.*, in press.

Dellino, P., Isaia, R., La Volpe, L. and Orsi, G. (2001). Statistical analysis of textural data from complex pyroclastic sequence: implication for fragmentation processes of the Agnano-Monte Spina eruption (4.1 ka), Phlegraean Fields, southern Italy. *Bull. Volcanol.* 63, 443-461.

Dellino, P., Isaia, R., La Volpe, L. and Orsi, G. (2004a). Interference of particles fallout on the emplacement of pyroclastic surge deposits of the Agnano-Monte Spina eruption (Phlegraean Fields, Southern Italy). *J. Volcanol. Geotherm. Res.*, in press.

Di Girolamo, P., Ghiara, M.R., Lirer, L., Munno, R., Rolandi, G.and Stanzione, D. (1984). Vulcanologia e petrologia dei Campi Flegrei. *Boll. Soc. Geol. It.* 103, 349-413.

Di Vito, M. A., Isaia, R., Orsi, G., Southon, J., de Vita, S., D'Antonio, M., Pappalardo, L. and Piochi, M. (1999). Volcanic and deformational history of the Campi Flegrei caldera in the past 12 ka. *J. Volcanol. Geotherm. Res.* 91, 221-246.

Di Vito, M. A., Lirer, L., Mastrolorenzo, G. and Rolandi, G. (1987). The Monte Nuovo eruption (Campi Flegrei, Italy). *Bull. Volcanol.* 49, 608-615.

Di Vito, M., D'Antonio, M., Braia, G., Carrol, M., Civetta, L., Isaia, R., Orsi, G., Piermattei, M. (2004). The Averno 2 eruption (Campi Flegrei caldera, Italy): influence of structural setting on magma evolution and eruption history. In prep.

Dubois, C. (1907). Pozzuoles Antique; Historie et topographie. Paris, Albert Fontemoing, 249-268.

Fedele, F., Giaccio, B., Isaia, R. and Orsi, G. (2003). The Campanian Ignimbrite eruption, Heinrich Event 4, and Palaeolithic change in Europe: a high-resolution investigation. *In* "Volcanism and Earth's Atmosphere", (A. Robok and C. Oppenheimer Ed.). AGU book, 139, 301-325.

Ferrucci, F., Gaudiosi, G., Pino, N. A. and Luongo, G. (1989). Seismic detection of a major moho upheaval beneath the Campania volcanic area (Naples, southern Italy). *Geophys. Res. Lett.* 16, 1317-1320.

Fisher, R.V. (1983). Flow transformations in sediment gravity flows. *Geology* 11, 273-274.

Volume n° 2 - from B16 to B33

Fisher, R.V., Orsi, G., Ort, M. and Heiken, G. (1993). Mobility of large-volume pyroclastic flow – emplacement of the Campanian Ignimbrite, Italy. *J. Volcanol. Geotherm. Res.* 56, 205-220.

Fulignati, P., Marianelli, P., and Sbrana,A. (1998). The 1944 eruption. *In* "Cities on volcanoes Field Excursion Guidebook" (G. Orsi, M.A. Di Vito and R. Isaia, Ed.), pp. 86-96. Osservatorio Vesuviano, Naples.

Giggenbach, W.F. (1987). Redox processes governing the chemistry of fumarolic gas discharges from White Island, New Zealand. *Applied Geochemistry* 2, 143-161.

Graham, D.W., Allard, P., Kilburn, C.R.J., Spera, F.J. and Lupton, J.E. (1993). Helium isotopes in some historical lavas from Mount Vesuvius. *J. Volcanol. Geotherm. Res.* 58, 359-366.

Granieri, D., Chiodini, G., Marzocchi, W., and Avino, R. (2003). Continuous monitoring of CO_2 soil diffuse degassing at Phlegraean Fields (Italy): influence of environmental and volcanic parameters. *Earth Planet. Sci. Lett.* 212, 167-179 .

Gurioli, L., Cioni, R., Sbrana, A. and Zanella, E. (2002). Transport and depositino of pyroclastic density currents over an inhabited area: the deposits of the AD 79 eruption of Vesuvius at Herculaneum, Italy. *Sedimentology* 49, 929-953.

Imbò, G. (1949). L'attività eruttiva vesuviana e relative osservazioni nel corso dell'intervallo intereruttivo 1906-1944 ed in particolare del parossismo eruttivo del marzo 1944. *Annali Oss. Vesuviano* serie V, 185-380.

Isaia, R., D'Antonio, M., Dell'Erba, F., Di Vito, M. A. and Orsi, G. (2004). The Astroni volcano: the only example of close eruptions within the same vent area in the recent history of of the Campi Flegrei caldera (Italy). *J. Volcanol. Geotherm. Res.,* in press.

Issel, A. (1883). Le oscillazioni lente del suolo o bradisismi. *Atti R. Univ. Genova*, IV:1-210.

Lajoie, J., Boudon, G. and Bourdier, J.L. (1989). Depositional mechanics of the 1902 pyroclastic nuée-ardente deposits of Mt. Pelée, Martinique. *J. Volcanol. Geotherm. Res.* 38, 131-142.

Lirer, L., Pescatore, T., Booth, P. and Walker, G. P. L. (1973). Two plinian pumice-fall deposits from Somma-Vesuvius, Italy. *Geol. Soc. of Am. Bull.* 84, 759-772.

Lundgren, P., Usai, S., Sansosti, E., Lanari, R., Tesauro, M., Eonaro, G. and Berardino, P. (2001). Modeling surface deformation observed with synthetic aperture interferometry at Campi Flegrei caldera. *J. Geophys. Research.* 106, 19355-19366.

Marianelli, P., Metrich, N. and Sbrana, A. (1999). Shallow and deep reservoirs involved in magma supply of the 1944 eruption of Vesuvius. *Bull. Volcanol.* 61, 48-63.

Marianelli, P., Metrich, N., Santacroce, R. and Sbrana, A. (1995). Mafic magma batches at Vesuvius: a glass inclusion approach to the modalities of feeding stratovolcanoes. *Contrib. Mineral. Petrol.* 120, 159-169.

Marotta, E. (2001). Processi deformativi all'interno di caldere risorgenti: analisi strutturale dell'isola d'Ischia e comparazione con altre aree risorgenti. PhD Thesis, pp 214. University of Naples, Italy.

Narcisi, B. and Vezzoli, L. (1999). Quaternary stratigraphy of distal tephra layers in the Mediterranean – an overview. *Global Planet. Change* 21, 31-50.

Orsi, G., Civetta, L., D'Antonio, M., Di Girolamo, P. and Piochi, M. (1995). Step-filling and development of a three-layers magma chamber: the Neapolitan Yellow Tuff case history. *J. Volcanol. Geotherm. Res*. 67, 291-312.

Orsi, G., Civetta, L., Del Gaudio, C., de Vita, S., Di Vito, M. A., Isaia, R., Petrazzuoli, S., Ricciardi, G. and Ricco, C. (1999a). Short-Term Ground Deformations and Seismicity in the Nested Campi Flegrei Caldera (Italy): an example of active block resurgence in a densely populated area. *J. Volcanol. Geotherm. Res.* 91, 415-451.

Orsi, G., D'Antonio, M., de Vita, S. and Gallo, G. (1992). The Neapolitan Yellow Tuff, a large-magnitude trachytic phreatoplinian eruption: eruptive dynamics, magma withdrawal and caldera collapse. *J. Volcanol. Geotherm. Res.* 53, 275-287.

Orsi, G., de Vita, S. and Di Vito, M. (1996). The restless, resurgent Campi Flegrei nested caldera (Italy): constraints on evolution and configuration. *J. Volcanol. Geotherm. Res.* 74, 179-214.

Orsi, G., de Vita, S., Di Vito, M., Nave, R. and Heiken, G. (2003a). Facing volcanic and related hazards in the Neapolitan area. *In* "Earth Sciences in the Cities: A Reader" (G. Heiken, R. Fakundiny, J. Sutter, Eds), pp. 121-170. Am. Geophys. Un., Sp. Publ. Series, Vol. 56, Washington.

Orsi, G., Di Vito, M.A. and Isaia, R. (2004b). Volcanic hazard assessment at the restless Campi Flegrei caldera. *Bull. Volcanol.,* in review.

Orsi, G., Gallo, G. and Zanchi, A. (1991). Simple shearing block resurgence in caldera depressions. A model from Pantelleria and Ischia. *J. Volcanol. Geotherm. Res.* 47, 1-11.

Orsi, G., Patella, D., Piochi, M. and Tramacere,

A. (1999b). Magnetic modeling of the Phlegraean Volcanic District with extension to the Ponza archipelago, Italy. *J. Volcanol. Geotherm. Res.* 91, 345-360.

Orsi, G., Petrazzuoli, S. and Wohletz, K. (1999c). The interplay of mechanical and thermo-fluid dynamical systems during an unrest episode in calderas: the Campi Flegrei caldera (Italy) case. *J. Volcanol. Geotherm. Res*. 91, 453-470.

Ort, M., Orsi, G., Pappalardo, L. and Fisher R.V. (2003). Anisotropy of magnetic susceptibility studies of depositional processes in the Campanian Ignimbrite, Italy. Bull. Volcanol. 65, 55-72.

Pappalardo, L., Civetta, L., D'Antonio, M., Deino, A., Di Vito, M. A., Orsi, G., Carandente, A., de Vita, S., Isaia, R. and Piochi, M. (1999). Chemical and isotopical evolution of the Phlegraean magmatic system before the Campanian Ignimbrite (37 ka) and the Neapolitan Yellow Tuff (12 ka) eruptions. *J. Volcanol. Geotherm. Res.* 91, 141-166.

Pappalardo, L., Civetta, L., de Vita, S., Di Vito, M., Orsi, G., Carandente, A., and Fisher R.V. (2002a). Timing of magma extraction during the Campanian Ignimbrite eruption (Campi Flegrei caldera). *J. Volcanol. Geotherm. Res.* 114, 479-497.

Pappalardo, L., Piochi, M., D'Antonio, M., Civetta, L. and Petrini R., (2002b). Evidence of multi-stage magmatic evolution deduced from Sr, Nd and Pb isotope data: the past 60 ka Campi Flegrei (Italy) history. *J. Petrol.* 43, 1415-1434.

Parancandola, A. (1947). I fenomeni bradisismici del Serapeo di Pozzuoli. Genovesi, Napoli.

Polacci, M., Pioli, L. and Rosi, M., (2003). The Plinian phase of the Campanian Ignimbrite eruption (phlegrean Fields, Italy): evidence from density measurements and textural characterization of pumice. *Bull. Volcanol.* 65, 418-432.

Rittmann, A. (1930). Geologie der Insel Ischia. Z. f. Vulkanol. Erganzungsband, 6.

Rittmann, A. (1950). Sintesi geologica dei Campi Flegrei. *Boll. Soc. Geol. It*. 69, 117-177.

Rolandi, G., Mastrolorenzo, G., Barrella, A. N. and Borrelli, A. (1993b). The Avellino Plinian Eruption of Somma-Vesuvius (3760 y.B.P.): the Progressive Evolution From Magmatic to Hydromagmatic Style. *J. Volcanol. Geotherm. Res.* 58, 67-88.

Rosi, M. and Santacroce, R. (1983). The A.D. 472 "Pollena" eruption: volcanological and petrological data for this poorly known plinian-type event at Vesuvius. *J. Volcanol. Geotherm. Res.* 17, 249-271.

Rosi, M. and Santacroce, R. (1984). Volcanic hazard assessment in the Phlegeran Fields: a contribution based on stratigraphic and historical data. *Bull. Volcanol.* 47(2), 359-370.

Rosi, M. and Sbrana, A. (1987). Phlegraean Fields. CNR Quad. de "La ric. sci." 114(9), pp. 167, Roma.

Rosi, M., Principe, C. and Vecci, R. (1993). The 1631 eruption of Vesuvius recunstructed from the review of chronichles and study of deposits. *J. Volcanol. Geotherm. Res.* 58, 151-182.

Rosi, M., Vezzoli, L., Castelmenzano, A. and Grieco, G. (1999). Plinian pumice fall deposit of the Campanian Ignimbrite eruption (Phlegraean Fields, Italy). *J. Volcanol. Geotherm. Res.* 91, 179-198.

Sansivero, F. (1999). Assetto stratigrafico ed evoluzione vulcanologica del settore orientale dell'isola d'Ischia negli ultimi 10 Ka. PhD Thesis, pp. 203, University of Naples, Italy.

Santacroce, R. (1983). A general model for the behavior of the Somma-Vesuvius volcanic complex. *J. Volcanol. Geotherm. Res.* 17, 237-248.

Seymour, K. and Christanis, K. (1995) Correlation of tephra layer in western Greece with a Late Pleistocene eruption in the Campanian province of Italy. *Quaternary Research* 43, 46-54.

Sigurdsson, H., Carey, S., Cornell, W. and Pescatore, T. (1985). The eruption of Vesuvius in 79 A.D.. *National Geographic Res.* 1, 332-387.

Tedesco, D. and Scarsi, P. (1999). Chemical (He, H_2, CH_4, Ne, Ar, N_2) and isotopic (He, Ne, Ar, C) variations at the Solfatara crater (Southern Italy): mixing of different sources in relation to seismic activity. *Earth and Planet. Sci.*171, 465– 480.

Thunnel, R., Federman, A., Sparks R.S.J. and Williams, D. (1979). The origin and volcanological significance of the Y-5 ash layer in the Mediterranean. *Quaternary Research* 12, 241-253.

Tonarini, S., Leeman, W.P., Civetta, L., D'antonio, M., Ferrara, G. and Necco, A. (2004). B/Nb and $\delta^{11}B$ systematics in the Phlegrean Volcanic District (PVD). *J. Volcanol. Geotherm. Res.*, in press.

Turi, B. and Taylor, H.P. (1976). Oxygen isotope studies of potassic volcanic rocks of the Roman Province, Central Italy. *Contrib. Mineral. Petrol.* 55, 1-31.

Vezzoli, L. (1988). Island of Ischia. CNR Quaderni de "La ricerca scientifica" 114 (10), pp. 122.

Wohletz, K., Orsi, G. and de Vita, S. (1995). Eruptive mechanisms of the Neapolitan Yellow Tuff interpreted from stratigraphic, chemical and granulometric data. *J. Volcanol. Geotherm. Res.* 67, 263-290.

Zollo, A., Judenherc, S., Virieux, J., Makris, J., Auger, E., Capuano, P., Chiarabba, C., De Franco, R.,

Volume n° 2 - from B16 to B33

Nichelini, A. and Musacchio, G. (2003). Tomographic imaging of the Campi Flegrei, Southern Italy, Caldera structure by high resolution active seismics. *EGS-AGU-EUG Joint Assembly*, Nice, France 6-11 April 2003, abstract.

Zollo, A., Marzocchi, W., Capuano, P., Lomax, A. and Iannaccone, G. (2002). Space and time behavior of seismic activity at Mt. Vesuvius volcano, Southern Italy. *Bull. Seism. Soc. Am.* 92, 625-640.

Back Cover:
field trip itinerary

FIELD TRIP MAP

Edited by APAT